

SYNTHESIS AND CHARACTERIZATION OF PLATINUM-ZIRCONIUM  
CATALYST SUPPORTED ON BICONTINUOUS LAMELLAR SILICA  
MORDENITE FOR *n*-HEXANE HYDROISOMERIZATION

MARYAM IBRAHIM

UNIVERSITI TEKNOLOGI MALAYSIA

SYNTHESIS AND CHARACTERIZATION OF PLATINUM-ZIRCONIUM  
CATALYST SUPPORTED ON BICONTINUOUS LAMELLAR SILICA  
MORDENITE FOR *n*-HEXANE HYDROISOMERIZATION

MARYAM IBRAHIM

A thesis submitted in fulfilment of the  
requirements for the award of the degree of  
Doctor of Philosophy

School of Chemical and Energy Engineering  
Faculty of Engineering  
Universiti Teknologi Malaysia

FEBRUARY 2020

## ACKNOWLEDGEMENT

In the name of Allah, the most gracious the most merciful, all praise and glory belongs to Allah for sustaining me through this programme. Peace and blessing to Prophet Muhammad S.A.W, his family and the entire muslim ummah. My profound gratitude to my supervisor Prof. Dr. Aishah Abdul Jalil for the immense knowledge, motivation, constructive criticism and friendship without whose support this research would not have been accomplished. I will also like to express my appreciation to my co-supervisor, Late Prof. Dr, Sugeng Triwahyono for his support, patience and guidance, may Allah S.W.T grant him aljanna firdaus as his final abode.

My sincere appreciation to all the Green Technology and Advanced Materials (GTAM) research group members for the never ending support and encouragement to complete task before dateline. I am also very grateful for the financial support by Tertiary Education Trust Fund (TETFund) through Abubakar Tafawa Balewa University Bauchi.

To my mum Hajiya Amita Ibrahim, thank you for your love, support and prayers throughout the entire period of this programme. May Allah S.W.T. continue to bless you with good health and long life. My endless gratitude to my dear brothers (Ibrahim, Musa, Ahmad and Abdulkadir) and sisters (Ya Halita, Amina, Zainab, Aisha, Amita, Hapsat and Jidda) for their love, encouragement and moral support. To my children Muhammad (Mubarak), Ibrahim (Abba), Musa, Maryam (Iman) and Fatima (Ihsan), thank you for your patience, understanding and striving hard to achieve your goals even in my absence, May Allah (S.W.T.) continue to bless you all.

Last but not the least, a million thanks to the Bamalam family, Alhaji Mijinyawa Jamare family, Chikaji family, Sadiya Alka and Zainab Jagun for their continuous support throughout the period of my study.

## ABSTRACT

Catalytic hydroisomerization of *n*-alkane has been one of the vital processes in the petroleum refining industry to improve the quality of gasoline. The existing catalysts have registered low isomerization performance due to the poor accessibility of active sites for the reactant molecules and the strong acid sites tend to be more selective towards cracking, thus affecting the overall efficiency of the process. This study investigated the catalytic performance of modified mordenite zeolite in *n*-hexane hydroisomerization. A novel protonated mordenite catalyst with bicontinuous lamellar morphology (HM@KCC-1) was successfully prepared via a microemulsion system with a mordenite seed-assisted crystallization technique. Platinum (Pt) was loaded by wet impregnation method and the catalytic performance was compared with Pt supported on commercial mordenite zeolite. The catalysts were characterized with X-ray diffraction, field emission scanning microscopy, transmission electron microscopy (TEM), surface area analyzer and electron spin resonance spectroscopy. The acidity was determined by pyridine and 2,6-lutidine adsorbed Fourier transformation infrared (FTIR) spectroscopy, while the catalytic performance was conducted in a microcatalytic pulse reactor at 150-350 °C under a hydrogen stream. The higher catalytic activity of Pt/HM@KCC-1 was achieved with 75% conversion, 98% isomer selectivity and 74% isomer yield compared to Pt/HM with 60% conversion, 40% isomer selectivity and 24% isomer yield at 300 °C. This was attributed to the well-dispersed Pt nanoparticles on the bicontinuous lamellar structure of HM@KCC-1 evidenced from the TEM images and the moderate acid sites on Pt/HM@KCC-1 as shown by FT-IR which favoured the dehydrogenation/hydrogenation function and the skeletal isomerization, respectively. Furthermore, the effect of zirconium (Zr) incorporation was investigated with different Zr loading (1, 5, 10wt %) on HM@KCC-1. The results showed formation of permanent Lewis acid sites which was selective towards the generation of mono-branched isomers. Hence, Zr has great potential as a promoter with 5Zr/HM@KCC-1 exhibiting the best catalytic performance. Zr as a promoter in Pt/5Zr-HM@KCC-1 was prepared by impregnation with 0.5wt % Pt. The isomer yield followed the order of Pt/5Zr-HM@KCC-1(86) > Pt/HM@KCC-1(74) > 5Zr-HM@KCC-1(60), best catalyst showed remarkable increased strength of Lewis acid sites and selectivity towards the di-branched isomer. Zr evidently enhanced the formation of molecular hydrogen-generated protonic acid sites which plays an important role in the hydroisomerization process. The optimum isomer yield for the *n*-hexane hydroisomerization obtained by response surface methodology was 85.7% at a reaction temperature of 293 °C, reduction temperature of 474 °C and flow of hydrogen over catalyst weight of 502 ml.g<sup>-1</sup>min<sup>-1</sup>. The experiment carried out at these optimum conditions yielded 84.1% isomer with 1.9% error. This study has highlighted the efficient design of Zr promoted Pt on HM@KCC-1 catalyst with appropriate metal/acid sites functions for hydroisomerization. In conclusion, the promising performance of PtZr/HM@KCC-1 catalyst demonstrated the potential to be used for the production of high-quality fuel, particularly for *n*-alkane hydroisomerization in the refining processes.

## ABSTRAK

Pengisomeran hidro n-alkana bermangkin telah menjadi salah satu proses penting dalam industri penapisan petroleum untuk meningkatkan kualiti petrol. Mangkin sedia ada telah mencatatkan prestasi isomerisasi yang rendah disebabkan oleh kebolehcapaian tapak aktif yang lemah untuk molekul reaktan dan tapak asid yang kuat lebih cenderung memilih terhadap keretakan, sekali gus menjejaskan kecekapan keseluruhan proses. Kajian ini dikendalikan untuk mengkaji prestasi pemangkin zeolit mordenit yang diubahsuai pada pengisomeran hidro n-heksana. Pemangkin mordenit berproton baharu dengan morfologi lamela dwiselanjar (HM@KCC-1) telah berjaya dihasilkan dengan menggunakan sistem mikroemulsi dengan dibantu oleh teknik penghabluran benih mordenit. Platinum (Pt) telah dimuatkan menerusi kaedah impregnasi basah dan prestasi pemangkinan telah dibandingkan dengan Pt yang disokong pada zeolit mordenit komersial. Mangkin-mangkin ini telah dicirikan dengan pembelauan sinar-X, mikroskopi elektron imbasan pancaran medan, mikroskopi penghantaran elektron (TEM), penganalisa luas permukaan dan spektroskopi resonans putaran elektron. Keasidan telah ditentukan menggunakan piridin dan 2,6-lutidin dijerap spektroskopi inframerah transformasi Fourier (FTIR), manakala prestasi pemangkinan dilakukan dalam reaktor denyut bermangkin mikro pada 150-350 °C dalam aliran hidrogen. Aktiviti pemangkinan yang lebih tinggi menggunakan Pt/HM@KCC-1 telah dicapai dengan 75% penukaran, 98% selektiviti isomer dan 74% hasil isomer berbanding Pt/HM dengan 60% penukaran, 40% selektiviti isomer dan 24% hasil isomer pada 300 °C. Ini adalah disebabkan oleh nanopartikel Pt yang tersebar dengan baik pada struktur lamela HM@KCC-1 yang dibuktikan daripada imej TEM dan tapak asid yang banyak di Pt/HM@KCC-1 seperti yang ditunjukkan oleh FTIR yang masing-masing cenderung terhadap fungsi nyah hidrogenasi /hidrogenasi dan isomerisasi rangka. Tambahan pula, kesan penggabungan zirkonium (Zr) telah diselidiki dengan kandungan muatan Zr yang berbeza (1,5,10% berat) pada HM@KCC-1. Keputusan menunjukkan pembentukan tapak asid Lewis kekal yang terpilih ke arah penghasilan isomer bercabang-satu. Oleh itu, Zr mempunyai potensi tinggi sebagai pengalok dengan 5Zr/HM@KCC-1 yang mempamerkan prestasi bermangkin terbaik. Zr sebagai pengalok dalam Pt/5Zr-HM@KCC-1 telah disediakan menggunakan impregnasi dengan 0.5% berat Pt. Hasil isomer mengikut susunan adalah Pt/5Zr-HM@KCC-1 (86)> Pt/HM@KCC-1 (74)> 5Zr-HM@KCC-1 (60), mangkin terbaik menunjukkan peningkatan kekuatan tapak asid Lewis dan selektiviti yang luar biasa terhadap isomer bercabang-dua. Zr terbukti meningkatkan pembentukan tapak asid proton yang dihasilkan oleh molekul hidrogen yang memainkan peranan penting dalam proses pengisomeran hidro. Hasil isomer optimum untuk pengisomeran hidro n-heksana yang diperolehi melalui kaedah gerakbalas permukaan adalah 85.7% pada suhu tindak balas 293 °C, suhu penurunan 474 °C dan aliran hidrogen ke atas berat mangkin, 502 ml.g<sup>-1</sup>min<sup>-1</sup>. Eksperimen yang dijalankan pada keadaan optimum ini menghasilkan 84.1% isomer dengan ralat 1.9%. Kajian ini menyerlahkan pembuatan Zr yang efisien dibantu oleh Pt pada mangkin HM@KCC-1 dengan fungsi tapak logam/asid yang sesuai untuk pengisomeran hidro. Kesimpulannya, prestasi mangkin PtZr/HM@KCC-1 yang menggalakkan menunjukkan potensi untuk digunakan dalam pengeluaran bahan api berkualiti tinggi, terutamanya untuk pengisomeran hidro n-alkana dalam proses penapisan.

## TABLE OF CONTENTS

	<b>TITLE</b>	<b>PAGE</b>
	<b>DECLARATION</b>	<b>iii</b>
	<b>DEDICATION</b>	<b>iv</b>
	<b>ACKNOWLEDGEMENT</b>	<b>v</b>
	<b>ABSTRACT</b>	<b>vi</b>
	<b>ABSTRAK</b>	<b>vii</b>
	<b>TABLE OF CONTENTS</b>	<b>viii</b>
	<b>LIST OF TABLES</b>	<b>xii</b>
	<b>LIST OF FIGURES</b>	<b>xiii</b>
	<b>LIST OF APPENDICES</b>	<b>xix</b>
<b>CHAPTER 1</b>	<b>INTRODUCTION</b>	<b>1</b>
	1.1 Research Background	1
	1.2 Problem Statement and Hypothesis	4
	1.3 Objectives of the Study	5
	1.4 Scope of the Study	6
	1.5 Significance of the Study	8
	1.6 Thesis Outline	8
<b>CHAPTER 2</b>	<b>LITERATURE REVIEW</b>	<b>9</b>
	2.1 Introduction	9
	2.2 Alkane Hydroisomerization	11
	2.3 Catalysis	14
	2.3.1 Homogenous Catalysis	14
	2.3.2 Heterogeneous Catalysis	14
	2.4 Catalyst for Hydroisomerization	15
	2.4.1 Zirconia-based Catalysts	16
	2.4.2 Zeolite-based Catalyst	18

2.4.2.1	Nature of Acidic Sites of Zeolite-Based Catalyst	21
2.4.2.2	Mesoporous Zeolites	22
2.4.2.3	Mordenite Zeolite	27
2.4.2.4	Silica modified zeolites	28
2.5	Hydroisomerization Mechanism	29
2.5.1	Bifunctional Mechanism	30
2.5.2	Acid Catalyzed Mechanism	30
2.6	Hydrogen Spillover	32
2.7	Hydroisomerization Thermodynamics	34
2.8	Evaluation of Mass transfer Parameters	35
2.9	Response Surface Methodology	36
2.10	Literature Summary	37
<b>CHAPTER 3</b>	<b>RESEARCH METHODOLOGY</b>	<b>39</b>
3.1	Preface	39
3.2	Chemicals and Materials	41
3.3	Preparation of catalysts	42
3.3.1	Preparation of Protonated Mordenite (HM) and Platinum Supported on Protonated Mordenite (Pt/HM)	42
3.3.2	Synthesis of Protonated Bicontinuous Lamellar Silica Mordenite (HM@KCC-1)	42
3.3.3	Preparation of Metal Supported on Protonated Bicontinuous Lamellar Silica Mordenite Catalysts	43
3.4	Catalysts Characterization	44
3.4.1	X-Ray Diffraction (XRD) Analysis	44
3.4.2	Surface Area and Pore Analysis	44
3.4.3	Morphology and Elemental Analysis	45
3.4.4	Ultraviolet Visible Spectroscopy (UV-Vis)	45
3.4.5	Fourier Transform Infrared (FTIR) Spectroscopy	45
3.4.5.1	Potassium Bromide (KBr) pellet Method	46

3.4.5.2	FTIR Study on Probing by Pyridine and 2,6-dimethylpyridine Adsorption	46
3.4.5.3	Generation of Protonic Acid Sites	47
3.4.5.4	In <i>situ</i> (H <sub>2</sub> +C <sub>6</sub> H <sub>14</sub> ) FTIR Spectroscopy	47
3.4.6	Electron Spin Resonance (ESR) Spectroscopy	47
3.4.7	Temperature Programmed Reduction (TPR)	48
3.5	Catalytic Testing	48
3.6	Optimization using Response Surface Methodology (RSM)	49
3.7	Stability Evaluation and Kinetic Study	51
<b>CHAPTER 4</b>	<b>RESULTS AND DISCUSSION</b>	<b>53</b>
4.1	Introduction	53
4.2	Effect of Incorporation of Bicontinuous Lamella Silica on Mordenite	53
4.2.1	Physicochemical Properties of Catalysts	53
4.2.2	Synthesis Mechanism for HM@KCC-1	68
4.2.3	Catalytic Performance	69
4.3	Preliminary Investigation on the Effect of Monometallic supported Catalysts	78
4.4	Effect of Zirconium loading on HM@KCC-1 in <i>n</i> -hexane Hydroisomerization	79
4.4.1	Physicochemical Properties of the Zirconium Loaded Catalysts	79
4.4.2	Catalytic Performance	91
4.5	Effect of Zr as promoter in PtZr/HM@KCC-1 as Catalyst for <i>n</i> -Hexane Hydroisomerization	93
4.5.1	Molecular Hydrogen-originated Protonic Acid Sites on PtZr/HM@KCC-1 (1-10 zirconium weight percent)	94
4.5.2	Catalytic Performance of PtZr/HM@KCC-1 (1-10 wt% Loading)	97
4.5.3	Mechanism for <i>n</i> -hexane Hydroisomerization over PtZr/HM@KCC-1	99



4.5.4	Comparison study of catalytic performance of different zeolite for <i>n</i> -hexane hydroisomerization	103
4.5.5	Process Optimization using Response Surface Methodology (RSM)	106
4.5.6	Stability Test	114
<b>CHAPTER 5</b>	<b>CONCLUSION AND RECOMMENDATIONS</b>	<b>115</b>
5.1	Conclusion	115
5.2	Future Works	117
	<b>REFERENCES</b>	<b>119</b>
	<b>Appendix A</b>	<b>139</b>
	<b>Calculation of Percentage of Platinum (Pt) and Zirconium (Zr)</b>	<b>139</b>
	<b>LIST OF PUBLICATIONS</b>	<b>149</b>

## LIST OF TABLES

TABLE NO	TITLE	PAGE
Table 2.1	RON of Hydrocarbon (Daly <i>et al.</i> , 2016)	13
Table 2.2	Advantages and disadvantages of heterogeneous reactions	15
Table 2.3	Structural details of conventional zeolites for isomerization of n-alkanes (O'Chonnor <i>et al.</i> , 1996)	18
Table 2.4	Various zeolite supports for hydroisomerization of n-alkanes	26
Table 2.5	Types of catalysts for C5-C6 paraffin hydrocarbon isomerization (Shakun <i>et al.</i> , 2014)	35
Table 3.1	List of chemicals	41
Table 3.2	Coded levels for independent parameters used in the experimental design	50
Table 3.3	Experimental design of n-hexane hydroisomerization	51
Table 4.1	Textural properties of HM and HM@KCC-1	57
Table 4.2	Acidity using pyridine FTIR	65
Table 4.3	Catalytic activity of mordenite-based catalysts for n-hexane hydroisomerization	75
Table 4.4	Textural properties of Zr modified HM@KCC-1 catalyst	83
Table 4.5	Textural properties of Zr promoted PtZr/HM@KCC-1	95
Table 4.6	Comparison study of catalytic performance of different zeolite for n-hexane hydroisomerization	106
Table 4.7	Experimental design and response values for different conditions	108
Table 4.8	Analysis of variance (ANOVA) test using 23 central composite design (CCD) for the isomer yield	109
Table 4.9	Comparison of predicted and observed responses at the optimum conditions obtained from RSM	114

## LIST OF FIGURES

FIGURE NO	TITLE	PAGE
Figure 2.1	World energy consumption by energy source (IEO, 2019)	10
Figure 2.2	The processing sequence in a modern refinery of high complexity, indicating major process flow between operations (modified from Gary, 1994)	12
Figure 2.3	Brønsted and Lewis acid structure (Hattori, 2010)	22
Figure 2.4	Structure and pore size of mordenite zeolite (Sano, 2001)	28
Figure 2.5	Acid-catalysed pathways of isomerization of n-hexane via monomolecular mechanism (Alazman et al., 2018)	32
Figure 2.6	Schematic illustration for molecular hydrogen-originated protonic acid site (modified from Triwahyono <i>et al.</i> , 2010)	34
Figure 2.7	Representation of the mass transfer process for the n-hexane hydroisomerization over catalyst pellet (modified from Jalil et al., 2019)	36
Figure 3.1	Research flow chart	40
Figure 3.2	Schematic diagram of the microcatalytic pulse reactor: 1-Regulator, 2- Valve, 3-Mass Flow Controller, 4-Mixing Chamber, 5-Fixed Bed Reactor, 6-Temperature Controller, 7- Gas Trap and 8-GC	49
Figure 4.1	XRD pattern for all catalysts	54
Figure 4.2	Nitrogen adsorption/desorption isotherm and pore size distribution for A) HM, B) Pt/HM, C) HM@KCC-1 and D) Pt/HM@KCC-1	56

Figure 4.3	(A) FESEM image of HM@KCC-1 and TEM images of HM@KCC-1 at different magnification (B) 100 nm, (C) 50 nm, and (D) 20 nm	58
Figure 4.4	FESEM images of commercial mordenite zeolite	59
Figure 4.5	High Resolution TEM images for Pt/HM@KCC-1 with different magnification of (A) 0.2 $\mu\text{m}$ , (B) 50 nm, (C) 5nm with FFT showing Pt lattice and (D) 5 nm with FFT showing silica lattice.	60
Figure 4.6	IR KBr spectra for (a) HM, (b) Pt/HM, (c) HM@KCC-1 and (d) Pt/HM@KCC-1 catalyst	61
Figure 4.7	IR spectra of hydroxyl group region for (a) HM, (b) Pt/HM, (c) HM@KCC-1 and (d) Pt/HM@KCC-1	62
Figure 4.8	Intensity of Gaussian peak for IR spectra of hydroxyl group region	62
Figure 4.9	FT-IR spectra of Pyridine adsorbed on (a) HM, (b) Pt/HM, (c) HM@KCC-1 and (d) Pt/HM@KCC-1	64
Figure 4.10	FT-IR spectra of 2,6-dimethylpyridine adsorbed on all studied catalysts (a) adsorbed onto (A) HM (B) Pt/HM, (C) Pt/HM@KCC-1 and outgassed at (b) room temperature, (c) 50 $^{\circ}\text{C}$ , (d) 75 $^{\circ}\text{C}$ , (e) 100 $^{\circ}\text{C}$ , (f) 125 $^{\circ}\text{C}$ , (g) 150 $^{\circ}\text{C}$ , (h) 175 $^{\circ}\text{C}$ and 200 $^{\circ}\text{C}$	68
Figure 4.11	ESR spectra of (a) HM, (b) Pt/HM, (c) HM@KCC-1 and (d) Pt/HM@KCC-1	69
Figure 4.12	Schematic illustration of the formation process of bicontinuous lamellar mordenite (HM@KCC-1)	70
Figure 4.13	Product distribution of <i>n</i> -hexane hydroisomerization in the presence of hydrogen	72
Figure 4.14	Bifunctional catalyzed pathway for <i>n</i> -hexane hydroisomerization over Pt/HM@KCC-1	73
Figure 4.15	Conversion rate of <i>n</i> -hexane, cyclohexane and <i>n</i> -heptane over Pt/HM@KCC-1	76
Figure 4.16	Catalytic performance of Pt/HM@KCC-1 in cyclohexane and <i>n</i> -heptane hydroisomerization.	77

Figure 4.17	Effect of different metal loading on n-hexane hydroisomerization in terms of isomer yield	79
Figure 4.18	XRD pattern for a) HM@KCC-1, b) 1Zr/HM@KCC-1, c) 5Zr/HM@KCC-1 and d) 10Zr/HM@KCC-1	81
Figure 4.19	(A) N <sub>2</sub> adsorption-desorption isotherms and (B) Pore size distribution for (a) HM@KCC-1, (b) 1Zr/HM@KCC-1, (c) 5Zr/HM@KCC-1 and (d) 10Zr/HM@KCC-1	82
Figure 4.20	FTIR KBr for a) HM@KCC-1 b) 1Zr/HM@KCC-1 c) 5Zr/HM@KCC-1 and d) 10Zr/HM@KCC-1	84
Figure 4.21	H <sub>2</sub> -TPR profiles of all Zr modified HM@KCC-1 catalyst	85
Figure 4.22	UV-Vis spectra of all studied catalysts	86
Figure 4.23	(A) IR spectra of hydroxyl region (B) Integrated area of hydroxyl group peaks (C) Lattice stretching at region 1500-2200 cm <sup>-1</sup> for (a) HM@KCC-1, (b) 1Zr/HM@KCC-1, (c) 5Zr/HM@KCC-1 and (d) 10Zr/HM@KCC-1	88
Figure 4.24	IR spectra of 2,6-dimethylpyridine adsorbed on activated (A) HM@KCC-1, (B) 1Zr/HM@KCC-1, (C) 5Zr/HM@KCC-1 (D) 10Zr/HM@KCC-1 (a) at room temperature, followed by heating in a vacuum at (b) 100 °C, (c) 150 °C and (d) 200°C	90
Figure 4.25	Changes in peak area for Brønsted and Lewis acid sites for Zr modified HM@KCC-1 catalysts	91
Figure 4.26	Catalytic Performance of Zr modified HM@KCC-1 in terms of A. Rate of Conversion and B. Isomer Yield	92

Figure 4.27	IR spectra of 2,6-lutidine adsorbed on (A) 1Zr/HM@KCC-1, (B) 5Zr/HM@KCC-1 and (C) 10Zr/HM@KCC-1. Spectral changes when 2,6-lutidine-preadsorbed sample was heated in hydrogen at (b) room temperature (c) 100 °C, (d) 150 °C, (e) 200 °C, (f) 250 °C, (g) 300 °C, ((h) 350 °C and (a) 2,6-lutidine adsorbed at room temperature	97
Figure 4.28	Catalytic Performance of Zr modified Pt/HM@KCC-1 catalyst	99
Figure 4.29	Schematic illustration of complex reaction for <i>n</i> -hexane hydroisomerization over bifunctional Pt/H-zeolite catalysts	100
Figure 4.30	Changes in IR spectra of vibrational lattice stretching frequency in the region of 3000-2800 cm <sup>-1</sup> (A) Pt1Zr/HM@KCC-1, (B) Pt5Zr/HM@KCC-1 and (C) Pt10Zr/HM@KCC-1 when catalysts were exposed to (a) hydrogen and hexane at room temperature followed by heating at (b) 150 °C) 200 °C, (d) 250 °C, 300 °C and (e) 350 °C and the corresponding deformation vibrational frequency in the region of 1750-1350 cm <sup>-1</sup> (D-F)	102
Figure 4.31	Proposed mechanism of <i>n</i> -hexane hydroisomerization over PtZr/HM@KCC-1 catalyst	103
Figure 4.32	Pareto chart of the isomer yield	110
Figure 4.33	Predicted versus Observed value plot for the model	111
Figure 4.34	Response surface plot of the combined reaction temperature and treatment temperature	112
Figure 4.35	Response surface plot of the combined reaction temperature and F/W	113
Figure 4.36	Response surface plot of the combined flow and treatment temperature	114
Figure 4.37	Stability Test	115

## LIST OF ABBREVIATIONS

AKI	-	Anti-knock Index
ANOVA	-	Analysis of variance
AR	-	Analytical grade
BET	-	Brunauer-Emmett-Teller
CCD	-	Central Composite Design
CTAB	-	Cetyltrimethylamminium bromide
DF	-	Degree of freedom
DFT	-	Density functional theory
DOE	-	Design of experiment
Ea	-	Activation energy
EG	-	Ethylene glycol
ESR	-	Electron Spin Resonance
FD	-	Factorial design
FESEM	-	Field Emission Scanning Electron Microscopy
FTIR	-	Fourier-Transform Infrared
GC	-	Gas Chromatography
IUPAC	-	International Union of Pure and Applied Chemistry
JCPDS	-	Joint Committee on Powder Diffraction Standards
KBr	-	Potassium Bromide
KCC-1	-	KAUST Catalytic Centre one
NLDFT	-	Non-local density functional theory
NMR	-	Nuclear magnetic resonance
RSM	-	Response surface methodology
SS	-	Sum of Squares
SSR	-	Sum of Squares Regression
TEM	-	Transmission Emission Spectroscopy
TEOS	-	Tetraethyl Orthosilicate
TPR	-	Temperature Programmed Reduction
UV-VIS	-	Ultra Violet Visible Spectrophometer
XRD	-	X-ray diffraction

## LIST OF SYMBOLS

nm	-	nanometer
wt %	-	weight percent
h	-	Hour
$2\theta$	-	Bragg angle
s	-	Second
$\lambda$	-	wavelength
W	-	Watts
g	-	gram
$^{\circ}\text{C}$	-	degree Celcius
min	-	minutes
K	-	Kelvin
mL	-	millilitre
P	-	pressure



## LIST OF APPENDICES

<b>APPENDIX</b>	<b>TITLE</b>	<b>PAGE</b>
Appendix A	Calculation of percentage of platinum (Pt) and Zirconium (Zr)	139
Appendix B	Raw data for n-hexane hydroisomerization	141
Appendix C	Calculation for catalytic activity	142
Appendix D	Calculation of rate constant, $k$	143
Appendix E	Calculation of acid sites concentration	145
Appendix F	Microcatalytic pulse reactor experimental set-up	146
Appendix G	Calculation of g-value	147
Appendix H	Calculation for mass transfer parameter	148

# CHAPTER 1

## INTRODUCTION

### 1.1 Research Background

Recently, global concern on the environment and health has led to new stringent legislative policies regarding gasoline. Gasoline contains mainly C4-C10 hydrocarbons, with a significant portion composed of linear alkanes. Although several processes such as catalytic cracking, reforming and alkylation have been employed to improve the octane number, current gasoline specifications being implemented worldwide impose a strong restriction on limiting the amount of aromatic and olefin compounds in gasoline (Zhang *et al.*, 2018a). Decreasing the quantity of these compounds has resulted in negative effects on the anti-knocking properties of gasoline that have to be compensated with other environmentally clean technologies. The need for high-quality gasoline has prompted a search for new technologies to improve the existing process in oil refineries and industries.

In this regard, the hydroisomerization of linear alkanes to branched isomers has generated great interest in modern refining industries. The process has proved to be an effective strategy to transform linear alkanes with a low octane number to their corresponding branched-isomers with a high octane number sufficient to improve fuel quality (Chica and Corma, 1999; Galadima and Muraza, 2015; Pinto *et al.*, 2016). Hydroisomerization is a better option compared with other technologies proven to be perilous to the environment.

The hydroisomerization of *n*-alkanes proceeds by the classical bifunctional metal-acid mechanism. It involves the de/hydrogenation of the *n*-alkane on the metal sites and the skeletal rearrangement of the intermediate alkenes on the acid sites (Ono, 2003). Besides, hydrogen plays a vital role in *n*-alkane hydroisomerization in the generation of protonic acid sites by the hydrogen spill-over phenomena (Triwahyono

*et al.*, 2007; Hattori, 2016). Hydrogen molecules split on the metal sites to form hydrogen atoms which then diffuse on the acid support and release their electrons to the Lewis acid sites, thereby forming protonic (Brønsted) acid sites. These acid sites participate in the reaction as the active sites, thus improving the catalytic performance (Hattori, 2016). Active protonic acid sites are involved in skeletal rearrangement to maintain high activity and stability of the catalysts (Li *et al.*, 2017). Besides, catalyst stability is also improved by the hydrogenation process to decrease coke deposition.

Several researchers have reported various types of acidic supports to include metal oxides and zeolites for the hydroisomerization process. Among which zeolites are the most promising due to their unique properties. Besides, different topologies of zeolite support such as SAPO-11, ZSM-22, ZSM-5, HY, HBEA and MOR have been widely applied for the hydroisomerization of *n*-alkanes. However, zeolites as support materials suffer several drawbacks which mainly include high diffusional limitation, easy catalyst deactivation and consequently low selectivity to bulky isomer products. Several strategies for the preparation of mesoporous zeolites have been reported, post-synthetic methods (top-down approach) such as demetallation which includes dealumination and desilication, hard-templating and soft-templating strategies (bottom-up approaches) (Schwieger *et al.*, 2016). Post-synthetic demetallation led to the loss of acidic sites by partial destruction of the zeolitic structure while the hard templating is expensive, often time-consuming and the constricted synthesis method is capable of not relinquishing any microporosity and acidity of parent zeolites during the formation of mesopores (Zhang and Ostraat, 2016). Soft-templating strategies represent the most attractive and efficient approach in the synthesis of mesoporous zeolites. It involves using surfactants which usually results in extensive mesoporosity with highly controllable structures. Thus, extensive efforts are being made to develop new catalysts with improved performance to achieve better mass transfer and a higher number of exposed active sites.

Typically, the mesoporous BEA (Musselwhite *et al.*, 2015), USY (Denayer *et al.*, 2000), ZSM-5 (Parsafard *et al.*, 2014), SAPO 11 (Zhang *et al.*, 2018a), ZSM-22 (Martens *et al.*, 2013) and even MOR (Monteiro *et al.*, 2014) were reported as good

hydroisomerization supports. However, these materials exhibited several drawbacks that include loss of acidity and low surface area.

Among the various zeolites with different topology which have been explored for hydroisomerization, mordenite zeolites with high thermal stability and tunable acidity has been very promising as supports in the hydroisomerization of *n*-alkanes (Monteiro *et al.*, 2014; Pastvova *et al.*, 2017; Pastvova, Pilar, Moravkova, Kaucky and Rathousky, 2018; Sazama *et al.*, 2018). Noble metals such as Pt, Pd and non-noble metals (Ni, Zn, Mo, Ga and Zr) have been utilized in *n*-alkane hydroisomerization. Particularly, Pt supported catalysts have been reported to be selective and stable in hydroisomerization. Accordingly, the isomerization of C6-C7 over Zr-Al-MCM-41 showed enhanced activity which was attributed to the appropriate proximity of Lewis acid sites that strengthened the strong Brønsted acid sites (Eswaramoorthi *et al.*, 2004). The isomerization selectivity to multibranched isomers for both *n*-hexane and *n*-heptane was higher for Zr containing Al-MCM-41 than Al-MCM-41 without zirconium.

Nonetheless, to date, there are no reports available regarding the modification of mordenite with bicontinuous concentric lamellar silica KCC-1 type material and incorporation of zirconium. In this thesis, bicontinuous lamella silica mordenite (HM@KCC-1) was used as the platinum support and *n*-hexane hydroisomerization was chosen as a model reaction. In addition, the physicochemical properties and catalyst activity of Pt/HM@KCCC-1 were compared with Pt/HM, since Pt is well known as an active noble metal for *n*-alkane hydroisomerization. The KCC-1 incorporation on mordenite modified the acidity to be moderate which facilitated the formation of isohexane in correlation with its catalytic activity. The presence of bicontinuous lamellar morphology and interparticle textural porosity contributing to a high surface area and large pore diameter of HM@KCC-1, which opens a new design possibility for a catalyst to with highly accessible active sites, which led to high selectivity towards isomerization suppressing the competing cracking reaction. Also, the influence of Zr as a promoter in *n*-hexane hydroisomerization was investigated by employing the bicontinuous concentric lamellar silica KCC-1 mordenite with zirconia. It was expected that the interaction of Zr with bicontinuous concentric lamellar silica

KCC-1 on mordenite would generate Lewis acid sites to improve the catalytic activity and selectivity. Further modification of Pt/HM@KCC-1 with zirconium to form PtZr/HM@KCC-1 was expected to enhance the hydroisomerization performance to obtain more di-branched isomers as it plays an important role in the generation of protonic acid sites via hydrogen spillover phenomena thus, enhancing the catalytic performance. The optimization of the *n*-hexane hydroisomerization process over PtZr/HM@KCC-1 was carried out using the response surface methodology (RSM).

## 1.2 Problem Statement and Hypothesis

In recent times, global energy demand has continued to increase due to the rapid growth in the world's population and the expansion of developing-world economies. Although fossil fuel will remain the major source of energy for the next few decades, environmental concerns have led to stringent policies to reformulate gasoline composition in order to improve fuel quality. The required quality of fuel can be achieved through progressive improvements in technology to increase product quality while minimizing undesirable effects on the environment. In an effort to address this problem, the hydroisomerization of linear alkanes has proved to be an effective industrial process to improve the octane number of gasoline. The product consists of branched alkanes with a considerably higher octane number than the corresponding linear alkanes. It is one of the key environmentally friendly processes employed to achieve high-quality clean gasoline, thereby meeting the required specifications of good fuel quality.

Industrial hydroisomerization catalysts are noble or transition metals supported on solid acids. These catalysts are bifunctional consisting of metallic and acidic functions. A suitable catalyst capable of high global conversion of *n*-alkanes and high selectivity to multi-branched isomers requires a proper choice of metal, as well as acidic functions for the hydroisomerization process. The current efficiency of refining and petrochemical industries is largely based on the use of highly active and durable catalysts, zeolites being the typical illustration of solid acids with large surface area as supports for developing environmentally benign processes. However, zeolite-based

catalysts suffer diffusional limitations and tend to be more selective towards the undesired cracking reaction because of their microporosity and strong acidity. Among the zeolite materials, mordenite is widely investigated in hydroisomerization due to its favourable properties such as high acidity, high thermal stability, shape selectivity, resistance to coke formation and high activity at moderate temperatures, but the hydroisomerization products are predominantly of mono-branched components, while the di-branched isomers are of essential importance for desired gasoline properties.

Recently considerable efforts have been made by researchers to improve the accessibility of active sites and molecular transport to and from active sites by introduction of micro-mesoporous materials. Although the development of hierarchical mordenite has been reported to enhance the diffusion of reacting species, the catalytic activity can still be improved by modifying the acidity to achieve a good balance in the metal/acid function. These are the two important parameters that can influence the extent of hydroisomerization reaction as well as the selectivity to the bulkier multi-branched products.

The main focus of this research is to design a new catalyst system to efficiently convert linear alkanes to high octane number branched alkanes. It was hypothesized that the incorporation of bicontinuous lamellar silica with mordenite could introduce mesoporosity to provide good accessibility of active sites and good metal dispersion as well as modify the acidity. This is due to the morphological changes, thus achieving suitable metal and acid functions in the dehydrogenation/hydrogenation and skeletal rearrangement in the hydroisomerization process. The addition of zirconium as a promoter would result in increased Lewis acidity which stabilizes the electron in the generation of protonic acid sites. These protonic acid sites could enhance the selectivity towards di-branched isomers.

### **1.3 Objectives of the Study**

The objectives of this study are:

1. To prepare and characterize bicontinuous lamellar silica mordenite and compare its performance with commercial mordenite as a support for platinum in *n*-hexane hydroisomerization.
2. To investigate the influence of zirconium loading on HM@KCC-1 and Pt/HM@KCC-1 and study the reaction mechanism over PtZr/HM@KCC-1 in *n*-hexane hydroisomerization.
3. To optimize the *n*-hexane hydroisomerization process using response surface methodology (RSM).

#### 1.4 Scope of the Study

This study is focused on designing hydroisomerization catalysts to solve the fundamental problems pertaining to low process efficiency. In this perspective, the effect of the incorporation of bicontinuous lamellar silica onto mordenite was compared with commercial mordenite as support for platinum, effect of zirconium loading on HM@KCC-1 and zirconium as a promoter on Pt/HM@KCC-1 in *n*-hexane hydroisomerization. Furthermore, the reaction mechanism and optimization of the *n*-hexane hydroisomerization process have been elucidated. The *n*-hexane hydroisomerization process efficiency is related to maximize the yield for multi-branched isomers thereby limiting the cracking selectivity. Therefore, the details of research scope are described as follows:

- (a) The effect of the incorporation of KCC-1 on mordenite and the comparison of its performance with commercial mordenite both with and without platinum was investigated in the hydroisomerization of *n*-hexane. In this study, bicontinuous lamellar silica mordenite was prepared as reported by previous protocols using water in oil microemulsion method with cetyltrimethylammonium bromide (CTAB) as a surfactant, butanol as a co-surfactant and toluene as the oil phase (Firminyansi *et al.*, 2016). Incipient wetness impregnation method was chosen to load 0.5 wt% Pt based on literature reports (Musselwhite *et al.*, 2016). The prepared catalysts were

characterized by X-Ray diffraction (XRD), N<sub>2</sub> physisorption, Field Emission Scanning Electron Microscope (FESEM) and Transmission Electron Microscope (TEM) in order to investigate the phase and crystal structure, surface area and pore size distribution and surface morphology and mesoporosity. Investigation of the nature and strength of acid sites was done by using Fourier Transform Infrared (FTIR) spectroscopy of preadsorbed pyridine, and 2,6-dimethylpyridine and the chemical environments was investigated by Electron Spin Resonance (ESR) Spectroscopy. Catalytic testing for *n*-hexane hydroisomerization was carried out at a temperature range of 150-350 °C under atmospheric pressure (Fatah *et al.*, 2016). However, this application is limited to the operative pressure of the fixed bed reactor is 1 atm.

- (b) The effect of zirconium loading on HM@KCC-1 and zirconium as a promoter on Pt/HM@KCC-1 in *n*-hexane hydroisomerization was investigated. A series of catalysts with different Zr loading (1, 5 and 10 wt %) were prepared using the incipient wetness impregnation method. The amount of zirconium was in the range stated based on literature (Triwahyono *et al.*, 2018) and preliminary studies on the catalytic activity evaluation using different zirconium loading. The prepared catalysts were characterized by XRD, N<sub>2</sub>-physisorption, FESEM, TEM and 2,6-dimethylpyridine-FTIR. Catalytic testing on *n*-hexane hydroisomerization was carried out at temperature range of 150-350 °C and at atmospheric pressure. The mechanism of *n*-hexane hydroisomerization over different zirconium loaded PtZr/HM@KCC-1 was studied using in situ 2,6-dimethylpyridine + H<sub>2</sub> (Izan *et al.*, 2018) and *n*-hexane + H<sub>2</sub> FTIR spectroscopy (Kondo *et al.*, 2007).
- (c) The optimal conditions for the *n*-hexane hydroisomerization process were determined by RSM using a Central Composite Design (CCD) developed by Statistica 6.0 StatSoft. The independent variables selected in the study are reaction temperature (250-350 °C), treatment temperature (400-500 °C) and flow of hydrogen over the weight of catalyst (475-525 ml/gmin) while the response is the isomer yield obtained from the catalytic performance evaluated in *n*-hexane hydroisomerization. These variables were selected based on the previous results from the literature and the preliminary analysis conducted



prior to the main study (Ruslan *et al.*, 2012, Fatah *et al.*, 2017, Setiabudi *et al.*, 2013).

## **1.5 Significance of the Study**

In this study, a novel catalyst, bicontinuous lamellar silica mordenite was prepared for the *n*-hexane hydroisomerization. As compared to the commercial mordenite, HM@KCC-1 has a bicontinuous lamellar morphology. This unique morphology modified the properties of the catalyst to have high thermal stability, moderate acidity and allows diffusion of bulky hydroisomerization products. A detailed comparison study on the property-activity relationship of Pt supported on HM/KCC-1 and HM was carried out. In addition, the effect of zirconium loading was investigated. Furthermore, the catalytic activity of PtZr/HM@KCC-1 and mechanism for *n*-hexane hydroisomerization was studied. Optimization by response surface methodology highlighted the factors affecting the hydroisomerization process. This study will have a significant contribution to scientific research and innovation, especially in the development of a new catalyst for *n*-alkane hydroisomerization.

## **1.6 Thesis Outline**

This thesis begins with Chapter one which described the research background, problem statement and hypothesis, objectives, scope and significance of the study. Chapter two reviewed the literature related to the catalysts and the recent progress on the hydroisomerization of *n*-alkanes. Chapter three described the step by step experimental procedure and characterization techniques for synthesized catalysts and *n*-hexane hydroisomerization. While chapter four presented data processing and discussion on physicochemical properties and catalytic performance of the catalysts. Finally, conclusions and recommendations for future research were highlighted in Chapter 5.

## REFERENCES

- Aboul-Gheit, A. K., & Awadallah, A. E. (2009). Effect of combining the metals of group VI supported on H-ZSM-5 zeolite as catalysts for non-oxidative conversion of natural gas to petrochemicals. *Journal of Natural Gas Chemistry*, 18(1), 71-77.
- Adzamic, Z., Adzamic, T., Muzic, M., & Sertic-Bionda, K. (2013). Optimization of the n-hexane isomerization process using response surface methodology. *Chemical Engineering Research and Design*, 91(1), 100-105.
- Afzal, S., Quan, X., Chen, S., Wang, J., & Muhammad, D. (2016). Synthesis of manganese incorporated hierarchical mesoporous silica nanosphere with fibrous morphology by facile one-pot approach for efficient catalytic ozonation. *Journal of Hazardous Materials*, 318, 308-318.
- Ahmed, M. H., Muraza, O., Galadima, A., Jamil, A. K., Shafei, E. N., Yamani, Z. H., & Choi, K. H. (2018). Hydrothermal Stabilization of Rich Al-BEA Zeolite by Post-Synthesis Addition of Zr for Steam Catalytic Cracking of n-Dodecane. *Energy & Fuels*, 32(4), 5501-5508.
- Aitani, A., Akhtar, M. N., Al-Khattaf, S., Jin, Y., Koseoglu, O., & Klein, M. T. (2019). Catalytic Upgrading of Light Naphtha to Gasoline Blending Components: A Mini Review. *Energy & Fuels*, 33(5), 3828-3843.
- Akhmedov, V. M., & Al-Khowaiter, S. H. (2007). Recent advances and future aspects in the selective isomerization of high n-Alkanes. *Catalysis Reviews*, 49(1), 33-139.
- Alazman, A., Belic, D., Kozhevnikova, E. F., & Kozhevnikov, I. V. (2018). Isomerisation of n-hexane over bifunctional Pt-heteropoly acid catalyst: Enhancing effect of gold. *Journal of Catalysis*, 357, 80-89.
- Aly, H. M., Moustafa, M. E., & Abdelrahman, E. A. (2012). Synthesis of mordenite zeolite in absence of organic template. *Advanced Powder Technology*, 23(6), 757-760.
- Annur, N. H. R., Jalil, A. A., Triwahyono, S., & Ramli, Z. (2013). Relating cumene hydrocracking activity to the acidic center of CrO<sub>3</sub>-ZrO<sub>2</sub>. *Journal of Molecular Catalysis A: Chemical*, 377, 162-172.

- Aziz, F. F. A., Jalil, A. A., Triwahyono, S., & Mohamed, M. (2018). Controllable structure of fibrous SiO<sub>2</sub>-ZSM-5 support decorated with TiO<sub>2</sub> catalysts for enhanced photodegradation of paracetamol. *Applied Surface Science*, 455, 84-95.
- Aziz, M. A. A., Jalil, A. A., Triwahyono, S., & Sidik, S. M. (2014). Methanation of carbon dioxide on metal-promoted mesostructured silica nanoparticles. *Applied Catalysis A: General*, 486, 115-122.
- Babitz, S. M., Williams, B. A., Miller, J. T., Snurr, R. Q., Haag, W. O., & Kung, H. H. (1999). Monomolecular cracking of n-hexane on Y, MOR, and ZSM-5 zeolites. *Applied Catalysis A: General*, 179(1-2), 71-86.
- Bae, C. and Kim, J. (2017). Alternative fuels for internal combustion engines. *Proceedings of the Combustion Institute*, 36(3), 3389-3413.
- Bi, Y., Xia, G., Huang, W., & Nie, H. (2015). Hydroisomerization of long chain n-paraffins: the role of the acidity of the zeolite. *RSC Advances*, 5(120), 99201-99206.
- Baertsch, C. D., *et al.* (2002). Genesis of Brønsted Acid Sites During Dehydration of 2-Butanol on Tungsten Oxide Catalysts. *Journal of Catalysis*, 205(1): 44-57.
- Bezerra, M. A., Santelli, R. E., Oliveira, E. P., Villar, L. S., & Escalera, L. A. (2008). Response surface methodology (RSM) as a tool for optimization in analytical chemistry. *Talanta*, 76(5), 965-977.
- Bolshakov, A., Romero Hidalgo, D. E., van Hoof, A. J., Kosinov, N., & Hensen, E. J. (2019). Mordenite nanorods prepared by an inexpensive pyrrolidine-based mesopore for alkane hydroisomerization. *ChemCatChem*.
- Chekantsev, N. V., Gyngazova, M. S., & Ivanchina, E. D. (2014). Mathematical modeling of light naphtha (C<sub>5</sub>, C<sub>6</sub>) isomerization process. *Chemical Engineering Journal*, 238, 120-128.
- Chen, D., Chen, Y., Guo, X., Tao, W., Wang, J., Gao, S., & Gao, J. (2018). Mesoporous silica nanoparticles with wrinkled structure as the matrix of myristic acid for the preparation of a promising new shape-stabilized phase change material via simple method. *RSC Advances*, 8(60), 34224-34231.
- Chen, J., Cai, T., Jing, X., Zhu, L., Zhou, Y., Xiang, Y., & Xia, D. (2016). Surface chemistry and catalytic performance of amorphous NiB/H $\beta$  catalyst for n-hexane isomerization. *Applied Surface Science*, 390, 157-166.

- Chen, Z., Xu, J., Fan, Y., Shi, G., & Bao, X. (2015). Reaction mechanism and kinetic modeling of hydroisomerization and hydroaromatization of fluid catalytic cracking naphtha. *Fuel Processing Technology*, 130, 117-126.
- Chen, K., Fang, H., Wu, S., Liu, X., Zheng, J., Zhou, S., Duan, X., Zhuang, Y., Chi Edman Tsang, S. and Yuan, Y. (2019) ‘CO<sub>2</sub> hydrogenation to methanol over Cu catalysts supported on La-modified SBA-15: The crucial role of Cu–LaOx interfaces’, *Applied Catalysis B: Environmental*. Elsevier, 251(August 2018), pp. 119–129.
- Chica, A., & Corma, A. (1999). Hydroisomerization of pentane, hexane, and heptane for improving the octane number of gasoline. *Journal of Catalysis*, 187(1), 167-176.
- Chmielewská, E. (2019). Natural Zeolites as Sustainable and Environmental Inorganic Resources over the History to Present. *General Chemistry*.
- Conti, J., Holtberg, P., Diefenderfer, J., LaRose, A., Turnure, J. T., & Westfall, L. (2016). *International energy outlook 2016 with projections to 2040* (No. DOE/EIA-0484 (2016)). USDOE Energy Information Administration (EIA), Washington, DC (United States). Office of Energy Analysis.
- Corma, A., Fornes, V., Pergher, S. B., Maesen, T. L., & Buglass, J. G. (1998). Delaminated zeolite precursors as selective acidic catalysts. *Nature*, 396(6709), 353.
- Cui, Q., Wang, S., Wei, Q., Mu, L., Yu, G., Zhang, T., & Zhou, Y. (2019). Synthesis and characterization of Zr incorporated small crystal size Y zeolite supported NiW catalysts for hydrocracking of vacuum gas oil. *Fuel*, 237(2018), 597–605.
- Dai, W., Wang, C., Tang, B., Wu, G., Guan, N., Xie, Z., Hunger, M., & Li, L. (2016). Lewis acid catalysis confined in zeolite cages as a strategy for sustainable heterogeneous hydration of epoxides. *Acs Catalysis*, 6(5), 2955-2964.
- Daly, S. R., Niemeyer, K. E., Cannella, W. J., & Hagen, C. L. (2016). Predicting fuel research octane number using Fourier-transform infrared absorption spectra of neat hydrocarbons. *Fuel*, 183, 359-365.
- del Campo, P., Beato, P., Rey, F., Navarro, M. T., Olsbye, U., Lillerud, K. P., & Svelle, S. (2018). Influence of post-synthetic modifications on the composition, acidity and textural properties of ZSM-22 zeolite. *Catalysis Today*, 299, 120-134.

- Denayer, J. F., Baron, G. V., Jacobs, P. A., & Martens, J. A. (2000). Competitive physisorption effects in hydroisomerisation of n-alkane mixtures on Pt/Y and Pt/USY zeolite catalysts. *Physical Chemistry Chemical Physics*, 2(5), 1007-1014.
- El Haskouri, J., Cabrera, S., Guillem, C., Latorre, J., Beltrán, A., Beltrán, D., Marcos, M.D., & Amorós, P. (2002). Atrane precursors in the one-pot surfactant-assisted synthesis of high zirconium content porous silicas. *Chemistry of Materials*, 14(12), 5015-5022.
- Emeis, C. A. (1993). Determination of Integrated Molar Extinction Coefficients for Infrared Bands of Pyridine Adsorbed on Solid Acid Catalysts. *Journal of Catalysis*, Vol. 141, pp. 347–354.
- Eswaramoorthi, I., Sundaramurthy, V., & Lingappan, N. (2004). Hydroisomerisation of C<sub>6</sub>–C<sub>7</sub>n-alkanes over Pt loaded zirconium containing Al–MCM-41 molecular sieves. *Microporous and Mesoporous Materials*, 71(1-3), 109-115.
- Fatah, N. A. A., Triwahyono, S., Jalil, A. A., Ahmad, A., & Abdullah, T. A. T. (2016). n-Heptane isomerization over mesostructured silica nanoparticles (MSN): Dissociative-adsorption of molecular hydrogen on Pt and Mo sites. *Applied Catalysis A: General*, 516, 135-143.
- Fatah, N. A. A., Triwahyono, S., Jalil, A. A., Salamun, N., Mamat, C. R., & Majid, Z. A. (2017). n-Heptane isomerization over molybdenum supported on bicontinuous concentric lamellar silica KCC-1: Influence of phosphorus and optimization using response surface methodology (RSM). *Chemical Engineering Journal*, 314, 650-659.
- Febriyanti, E., Suendo, V., Mukti, R. R., Prasetyo, A., Arifin, A. F., Akbar, M. A., Triwahyono, S. & Marsih, I. N. (2016). Further insight into the definite morphology and formation mechanism of mesoporous silica KCC-1. *Langmuir*, 32(23), 5802-5811.
- Fihri, A., Cha, D., Bouhrara, M., Almaná, N., & Polshettiwar, V. (2012). Fibrous Nano-Silica (KCC-1)-Supported Palladium Catalyst: Suzuki Coupling Reactions Under Sustainable Conditions. *ChemSusChem*, 5(1), 85-89.
- Firmansyah, M. L., Jalil, A. A., Triwahyono, S., Hamdan, H., Salleh, M. M., Ahmad, W. F. W., & Kadja, G. T. M. (2016). Synthesis and characterization of fibrous silica ZSM-5 for cumene hydrocracking. *Catalysis Science & Technology*, 6(13), 5178-5182.

- Galadima, A., & Muraza, O. (2015). Hydroisomerization of sustainable feedstock in biomass-to-fuel conversion: a critical review. *International Journal of Energy Research*, 39(6), 741-759.
- Galadima, A., et al. (2009). Solid Acid Catalysts in Heterogeneous N-Alkanes Hydroisomerisation for Increasing Octane Number of Gasoline. *Science World Journal*, 4(3).
- Gao, L., Shi, Z., Etim, U. J., Wu, P., Han, D., Xing, W., Bai, P., & Yan, Z. (2019). Beta-MCM-41 micro-mesoporous catalysts in the hydroisomerization of n-heptane: Definition of an indexed isomerization factor as a performance descriptor. *Microporous and Mesoporous Materials*, 277, 17-28.
- García, J. R., et al. 2017. "Diffusion Controlled Lhw Kinetics. Simultaneous Determination of Chemical Kinetic and Equilibrium Adsorption Constants by Using the Weisz-Prater Approach." *Chemical Engineering Science*, 172: 444-452.
- Gary, J. H. Petroleum Refining: Technology and Economics, Chapter 4, Crude Distillation, 1994: Marcel Dekker, Inc., New York.
- Geng, L., Gong, J., Qiao, G., Ye, S., Zheng, J., Zhang, N., & Chen, B. (2019). Effect of Metal Precursors on the Performance of Pt/SAPO-11 Catalysts for n-Dodecane Hydroisomerization. *ACS Omega*, 4(7), 12598-12605.
- Ghani, N. N. M., Jalil, A. A., Triwahyono, S., Aziz, M. A. A., Rahman, A. F. A., Hamid, M. Y. S., Izan, S.M. & Nawawi, M. G. M. (2019). Tailored mesoporosity and acidity of shape-selective fibrous silica beta zeolite for enhanced toluene co-reaction with methanol. *Chemical Engineering Science*, 193, 217-229.
- Gong, S., Chen, N., Nakayama, S., & Qian, E. W. (2013). Isomerization of n-alkanes derived from jatropha oil over bifunctional catalysts. *Journal of Molecular Catalysis A: Chemical*, 370, 14-21.
- Guisnet, M. (2013). "Ideal" bifunctional catalysis over Pt-acid zeolites. *Catalysis Today*, 218, 123-134.
- Guisnet, M., Alvarez, F., Giannetto, G., & Perot, G. (1987). Hydroisomerization and hydrocracking of n-heptane on Pth zeolites. Effect of the porosity and of the distribution of metallic and acid sites. *Catalysis Today*, 1(4), 415-433.
- Guisnet, M., Fouche, V., Belloum, M., Bournonville, J. P., & Travers, C. (1991). Isomerization of n-hexane on platinum dealuminated mordenite catalysts I.

- Influence of the silicon-to-aluminium ratio of the zeolite. *Applied Catalysis*, 71(2), 283-293.
- Gustafsson, H., Isaksson, S., Altskär, A., & Holmberg, K. (2016). Mesoporous silica nanoparticles with controllable morphology prepared from oil-in-water emulsions. *Journal of Colloid and Interface Science*, 467, 253-260.
- Hamid, M. Y. S., Firmansyah, M. L., Triwahyono, S., Jalil, A. A., Mukti, R. R., Febriyanti, E., Suendo, V., Setiabudi, H.D., Mohamed, M.& Nabgan, W. (2017). Oxygen vacancy-rich mesoporous silica KCC-1 for CO<sub>2</sub> methanation. *Applied Catalysis A: General*, 532, 86-94.
- Hasan, M., Mohamed, A. M., Al-Kandari, H. (2018). Semi-industrial studies of Tungsten-based catalyst for hydroisomerization/ hydrocracking of n-hexane and n-heptane. *Molecular Catalysis*, 452, 1–10.
- Hattori, H. (2010). Solid acid catalysts: roles in chemical industries and new concepts. *Topics in Catalysis*, 53(7-10), 432-438.
- Hattori, H., & Shishido, T. (1997). Molecular hydrogen-originated protonic acid site as active site on solid acid catalyst. *Catalysis Surveys from Asia*, 1(2), 205-213..
- Hattori, H., *et al.* (2003). *Participation of the Protonic Acid Sites Originating from Molecular Hydrogen in Alkane Skeletal Isomerization Catalyzed by Pt/Wo<sub>3</sub>-Zro<sub>2</sub>*, Sapporo 060-8628, Japan. Paper presented at the Proceedings of 3rd Saudi-Japanese Catalyst Symposium, Dhahran.
- Hattori, H. (2016). *ChemInform Abstract : Solid Acid Catalysts : Roles in Chemical Industries and Solid Acid Catalysts : Roles in Chemical Industries and New Concepts*.
- He, J., Zhu, L., Liu, C., & Bai, Q. (2019). Optimization of the oil agglomeration for high-ash content coal slime based on design and analysis of response surface methodology (RSM). *Fuel*, 254, 115560.
- Hernández-Pichardo, M. L., & Macías-Salinas, R. (2016). Modeling the n-Hexane Isomerization over Iron Promoted Pt/WO<sub>x</sub>-ZrO<sub>2</sub> Catalysts Using Artificial Neural Networks. *Industrial & Engineering Chemistry Research*, 55(32), 8883-8889.
- Hino, M., & Arata, K. (1988). Synthesis of solid superacid of tungsten oxide supported on zirconia and its catalytic action for reactions of butane and pentane. *Journal of the Chemical Society, Chemical Communications*, (18), 1259-1260.

- Huyen, P. T., Nam, L. T., Vinh, T. Q., Martínez, C., & Parvulescu, V. I. (2018). ZSM-5/SBA-15 versus Al-SBA-15 as supports for the hydrocracking/hydroisomerization of alkanes. *Catalysis Today*, 306, 121-127.
- Iglesias, J., Melero, J. A., Morales, G., Paniagua, M., Hernández, B., Osatiashtiani, A., Lee, A. F and Wilson, K. (2018). ZrO<sub>2</sub>-SBA-15 catalysts for the one-pot cascade synthesis of GVL from furfural. *Catalysis Science and Technology*, 8(17), 4485–4493.
- Im, J., Shin, H., Jang, H., Kim, H., & Choi, M. (2014). Maximizing the catalytic function of hydrogen spillover in platinum-encapsulated aluminosilicates with controlled nanostructures. *Nature communications*, 5, 3370..
- Intarapong, P., Iangthanarat, S., Phanthong, P., Luengnaruemitchai, A., & Jai-In, S. (2013). Activity and basic properties of KOH/mordenite for transesterification of palm oil. *Journal of Energy Chemistry*, 22(5), 690-700.
- Ivanov, P., & Papp, H. (2000). FT-IR Study of the Isomerization of n-Butene over Different Zeolites. *Langmuir*, 16(20), 7769-7772.
- Ivanova, I. I., Kuznetsov, A. S., Knyazeva, E. E., Fajula, F., Thibault-Starzyk, F., Fernandez, C., & Gilson, J. P. (2011). Design of hierarchically structured catalysts by mordenites recrystallization: Application in naphthalene alkylation. *Catalysis Today*, 168(1), 133-139.
- Izan, S. M., Triwahyono, S., Jalil, A. A., Majid, Z. A., Fatah, N. A. A., Hamid, M. Y. S., & Ibrahim, M. (2019). Additional Lewis acid sites of protonated fibrous silica@ BEA zeolite (HSi@ BEA) improving the generation of protonic acid sites in the isomerization of C<sub>6</sub> alkane and cycloalkanes. *Applied Catalysis A: General*, 570, 228-237.
- Jalil, A. A., Gambo, Y., Ibrahim, M., Abdulrasheed, A. A., Hassan, N. S., Nawawi, M. G. M., Asli, U.A., Hassim, M.H. & Ahmad, A. (2019). Platinum-promoted fibrous silica Y zeolite with enhanced mass transfer as a highly selective catalyst for n-dodecane hydroisomerization. *International Journal of Energy Research*.
- Jaroszewska, K., Fedyna, M., & Trawczyński, J. (2019). Hydroisomerization of long-chain n-alkanes over Pt/AlSBA-15+ zeolite bimodal catalysts. *Applied Catalysis B: Environmental*, 255, 117756.
- Jiménez, C., Romero, F. J., Roldán, R., Marinas, J. M., & Gómez, J. P. (2003). Hydroisomerization of a hydrocarbon feed containing n-hexane, n-heptane and



- cyclohexane on zeolite-supported platinum catalysts. *Applied Catalysis A: General*, 249(1), 175-185.
- Kamarudin, N. H. N., Jalil, A. A., Triwahyono, S., Mukti, R. R., Ab Aziz, M. A., Setiabudi, H. D., Muhid, M.N.M. & Hamdan, H. (2012). Interaction of Zn<sup>2+</sup> with extraframework aluminum in HBEA zeolite and its role in enhancing n-pentane isomerization. *Applied Catalysis A: General*, 431, 104-112.
- Kang, J. S., Lim, J., Rho, W.-Y., Kim, J., Moon, D.-S., Jeong, J., Jung, D., Choi, J.W., Lee, J.K. Sung, Y.-E. (2016). Wrinkled silica/titania nanoparticles with tunable interwrinkle distances for efficient utilization of photons in dye-sensitized solar cells. *Scientific Reports*, 6, 30829.
- Karakoulia, S. A., Heracleous, E., & Lappas, A. A. (2019). Mild hydroisomerization of heavy naphtha on mono-and bi-metallic Pt and Ni catalysts supported on Beta zeolite. *Catalysis Today*.
- Katada, N., Suzuki, K., Noda, T., Miyatani, W., Taniguchi, F., & Niwa, M. (2010). Correlation of the cracking activity with solid acidity and adsorption property on zeolites. *Applied Catalysis A: General*, 373(1-2), 208-213.
- Kaucký, D., Sazama, P., Sobalík, Z., Hidalgo, J. M., Černý, R., & Bortnovský, O. (2015). Impact of Parent Zirconia Crystallinity/Amorphylicity on the n-heptane Isomerization over Pt/WO<sub>3</sub>-ZrO<sub>2</sub> Catalysts. *British Journal of Applied Science & Technology*, 10, 1-15.
- Khan, N. A., Kennedy, E. M., Dlugogorski, B. Z., Adesina, A. A., & Stockenhuber, M. (2018). A proposed reaction mechanism for the selective oxidation of methane with nitrous oxide over Co-ZSM-5 catalyst forming synthesis gas (CO+ H<sub>2</sub>). *International Journal of Hydrogen Energy*, 43(29), 13133-13144.
- Khitev, Y. P., Ivanova, I. I., Kolyagin, Y. G., & Ponomareva, O. A. (2012). Skeletal isomerization of 1-butene over micro/mesoporous materials based on FER zeolite. *Applied Catalysis A: General*, 441, 124-135.
- Kim, M. Y., Lee, K., & Choi, M. (2014). Cooperative effects of secondary mesoporosity and acid site location in Pt/SAPO-11 on n-dodecane hydroisomerization selectivity. *Journal of Catalysis*, 319, 232-238.
- Knaeble, W., & Iglesia, E. (2016). Acid strength and metal-acid proximity effects on methylcyclohexane ring contraction turnover rates and selectivities. *Journal of Catalysis*, 344, 817-830.

- Kondo, J. N., Yang, S., Zhu, Q., Inagaki, S., & Domen, K. (2007). In situ infrared study of n-heptane isomerization over Pt/H-beta zeolites. *Journal of Catalysis*, 248(1), 53-59.
- Konnov, S. V., Ivanova, I. I., Ponomareva, O. A., & Zaikovskii, V. I. (2012). Hydroisomerization of n-alkanes over Pt-modified micro/mesoporous materials obtained by mordenite recrystallization. *Microporous and Mesoporous Materials*, 164, 222-231.
- Kulawong, S., Prayoonpokarach, S., Neramittagapong, A., & Wittayakun, J. (2011). Mordenite modification and utilization as supports for iron catalyst in phenol hydroxylation. *Journal of Industrial and Engineering Chemistry*, 17(2), 346–351.
- Kurniawan, T., Muraza, O., Bakare, I. A., Sanhoob, M. A., & Al-Amer, A. M. (2018). Isomerization of n-butane over cost-effective mordenite catalysts fabricated via recrystallization of natural zeolites. *Industrial & Engineering Chemistry Research*, 57(6), 1894-1902.
- Le, X., Dong, Z., Liu, Y., Jin, Z., Huy, T.-D., Le, M., & Ma, J. (2014). Palladium nanoparticles immobilized on core–shell magnetic fibers as a highly efficient and recyclable heterogeneous catalyst for the reduction of 4-nitrophenol and Suzuki coupling reactions. *Journal of Materials Chemistry A*, 2(46), 19696-19706.
- Lee, J. K., & Rhee, H. K. (1997). Characteristics of Pt/H-beta and Pt/H-mordenite catalysts for the isomerization of n-hexane. *Catalysis Today*, 38(2), 235-242.
- Leofanti, G., Padovan, M., Tozzola, G., & Venturelli, B. (1998). Surface area and pore texture of catalysts. *Catalysis Today*, 41(1–3), 207–219.
- Lercher, J. A., Gründling, C., & Eder-Mirth, G. (1996). Infrared studies of the surface acidity of oxides and zeolites using adsorbed probe molecules. *Catalysis Today*, 27(3-4), 353-376.
- Li, G., Gao, L., Sheng, Z., Zhan, Y., Zhang, C., Ju, J., Zhang, Y., & Tang, Y. (2019). A Zr-Al-Beta zeolite with open Zr (iv) sites: an efficient bifunctional Lewis–Brønsted acid catalyst for a cascade reaction. *Catalysis Science & Technology*, 9(15), 4055-4065.
- Li, H., Liu, C., Wang, Y., Zheng, J., Fan, B., & Li, R. (2018a). Synthesis, characterization and n-hexane hydroisomerization performances of Pt

- supported on alkali treated ZSM-22 and ZSM-48. *RSC Advances*, 8(51), 28909-28917.
- Li, J., Liu, M., Guo, X., Dai, C., & Song, C. (2018b). Fluoride-mediated nano-sized high-silica ZSM-5 as an ultrastable catalyst for methanol conversion to propylene. *Journal of Energy Chemistry*, 27(4), 1225-1230.
- Li, W., Chi, K., Liu, H., Ma, H., Qu, W., Wang, C., Lv, G., & Tian, Z. (2017). Skeletal isomerization of n-pentane: A comparative study on catalytic properties of Pt/WO<sub>x</sub>-ZrO<sub>2</sub> and Pt/ZSM-22. *Applied Catalysis A: General*, 537, 59-65.
- Liu, S., He, Y., Zhang, H., Chen, Z., Lv, E., Ren, J., Yun, Y., Wen, X., & Li, Y.-W. (2019). Design and synthesis of Ga-doped ZSM-22 zeolites as highly selective and stable catalysts for n-dodecane isomerization. *Catalysis Science & Technology*.
- Liu, S., Ren, J., Zhang, H., Lv, E., Yang, Y., & Li, Y. W. (2016). Synthesis, characterization and isomerization performance of micro/mesoporous materials based on H-ZSM-22 zeolite. *Journal of Catalysis*, 335, 11-23.
- Lu, X., Guo, Y., Xu, C., Ma, R., Wang, X., Wang, N., Fu, Y. and Zhu, W. (2019). Preparation of mesoporous mordenite for the hydroisomerization of n - hexane. *Catalysis Communications*, 125(3), 21–25.
- Lyu, Y., Yu, Z., Yang, Y., Zhao, X., Wang, X., Liu, X., Mintova, S., Yan, Z. (2019a). Metal-acid balance in the in-situ solid synthesized Ni/SAPO-11 catalyst for n-hexane hydroisomerization. *Fuel*, 243, 398–405.
- Lyu, Y., Yu, Z., Yang, Y., Liu, L., Zhao, X., Liu, X., Mintova, S., Yan, Z., Zhao, G. (2019b). Metal and acid sites instantaneously prepared over Ni/SAPO-11 bifunctional catalyst. *Journal of Catalysis*, 374, 208–216.
- Ma, Z., Meng, X., Liu, N., & Shi, L. (2018). Pd-Ni doped sulfated zirconia: Study of hydrogen spillover and isomerization of N-hexane. *Molecular Catalysis*, 449, 114-121.
- Martens, J. A., Verboekend, D., Thomas, K., Vanbutsele, G., Gilson, J. P., & Pérez-Ramírez, J. (2013). Hydroisomerization of emerging renewable hydrocarbons using hierarchical Pt/H-ZSM-22 catalyst. *ChemSusChem*, 6(3), 421-425.
- Matsushashi, H., Shibata, H., Nakamura, H., & Arata, K. (1999). Skeletal isomerization mechanism of alkanes over solid superacid of sulfated zirconia. *Applied Catalysis A: General*, 187(1), 99-106.

- Maxwell, I. E. (1987). Zeolite catalysis in hydroprocessing technology. *Catalysis Today*, 1(4), 385-413.
- McCue, A. J., Mutch, G. A., McNab, A. I., Campbell, S., & Anderson, J. A. (2016). Quantitative determination of surface species and adsorption sites using Infrared spectroscopy. *Catalysis Today*, 259, 19-26.
- Meunier, F. C., Domokos, L., Seshan, K., & Lercher, J. A. (2002). In situ IR study of the nature and mobility of sorbed species on H-FER during but-1-ene isomerization. *Journal of Catalysis*, 211(2), 366-378.
- Monteiro, R., Ania, C. O., Rocha, J., Carvalho, A., & Martins, A. (2014). Catalytic behavior of alkali-treated Pt/HMOR in n-hexane hydroisomerization. *Applied Catalysis A: General*, 476, 148-157.
- Morterra, C., Cerrato, G., & Meligrana, G. (2001). Revisiting the use of 2, 6-dimethylpyridine adsorption as a probe for the acidic properties of metal oxides. *Langmuir*, 17(22), 7053-7060.
- Mouli, K. C., Sundaramurthy, V., Dalai, A. K., & Ring, Z. (2007). Selective ring opening of decalin with Pt-Ir on Zr modified MCM-41. *Applied Catalysis A: General*, 321(1), 17-26.
- Musselwhite, N., Na, K., Sabyrov, K., Alayoglu, S., & Somorjai, G. A. (2015). Mesoporous aluminosilicate catalysts for the selective isomerization of n-Hexane: the roles of surface acidity and platinum metal. *Journal of the American Chemical Society*, 137(32), 10231-10237.
- Na, K., Choi, M., & Ryoo, R. (2013). Recent advances in the synthesis of hierarchically nanoporous zeolites. *Microporous and Mesoporous Materials*, 166, 3-19.
- Nabgan, B., Abdullah, T. A. T., Tahir, M., Nabgan, W., Gambo, Y., Ibrahim, M., Saeh, I. & Moghadamian, K. (2017). Evaluation of theoretical and experimental mass transfer limitation in steam reforming of phenol-PET waste to hydrogen production over Ni/La-promoted Al<sub>2</sub>O<sub>3</sub> catalyst. *Journal of Environmental Chemical Engineering*, 5(3), 2752-2760.
- Narayanan, S., Vijaya, J. J., Sivasanker, S., Alam, M., Tamizhdurai, P., & Kennedy, L. J. (2015). Characterization and catalytic reactivity of mordenite—investigation of selective oxidation of benzyl alcohol. *Polyhedron*, 89, 289-296.

- Nishitoba, T., Yoshida, N., Kondo, J. N., & Yokoi, T. (2018). Control of Al Distribution in the CHA-Type Aluminosilicate Zeolites and Its Impact on the Hydrothermal Stability and Catalytic Properties. *Industrial & Engineering Chemistry Research*, 57(11), 3914-3922.
- O'Connor, C. T., Van Steen, E., & Dry, M. E. (1996). New catalytic applications of zeolites for petrochemicals. In *Studies in Surface Science and Catalysis* (Vol. 102, pp. 323-362): Elsevier.
- Oloye, F. F., Aliyev, R., & Anderson, J. A. (2018). Hydroisomerisation of n-heptane over Pt/sulfated zirconia catalyst at atmospheric pressure. *Fuel*, 222, 569-573.
- Ono, Y. (2003). A survey of the mechanism in catalytic isomerization of alkanes. *Catalysis Today*, 81(1), 3-16.
- Pacchioni, G., & Freund, H. J. (2018). Controlling the charge state of supported nanoparticles in catalysis: lessons from model systems. *Chemical Society Reviews*, 47(22), 8474-8502.
- Parry, E. P. (1963). An infrared study of pyridine adsorbed on acidic solids. Characterization of surface acidity. *Journal of Catalysis*, 2(5), 371-379.
- Parsafard, N., Peyrovi, M. H., & Rashidzadeh, M. (2014). n-Heptane isomerization on a new kind of micro/mesoporous catalyst: Pt supported on HZSM-5/HMS. *Microporous and Mesoporous Materials*, 200, 190-198.
- Pastvova, J., Kaucky, D., Moravkova, J., Rathousky, J., Sklenak, S., Vorokhta, M., Brabec, L., Pilar, R., Jakubec, I., Tabor, E., & Tabor, E. (2017). Effect of enhanced accessibility of acid sites in micromesoporous mordenite zeolites on hydroisomerization of n-hexane. *Acs Catalysis*, 7(9), 5781-5795.
- Pastvova, J., Pilar, R., Moravkova, J., Kaucky, D., Rathousky, J., Sklenak, S., & Sazama, P. (2018). Tailoring the structure and acid site accessibility of mordenite zeolite for hydroisomerisation of n-hexane. *Applied Catalysis A: General*, 562, 159-172.
- Peng, H. G., Xu, L., Wu, H., Zhang, K., & Wu, P. (2013). One-pot synthesis of benzamide over a robust tandem catalyst based on center radially fibrous silica encapsulated TS-1. *Chemical Communications*, 49(26), 2709-2711.
- Philippaerts, A., Paulussen, S., Turner, S., Lebedev, O. I., Van Tendeloo, G., Poelman, H., Bulut, M., De Clippel, F., Smeets, P., Sels, B. & Jacobs, P. (2010). Selectivity in sorption and hydrogenation of methyl oleate and elaidate on MFI zeolites. *Journal of Catalysis*, 270(1), 172-184.

- Pinto, T., Arquillière, P., Dufaud, V., & Lefebvre, F. (2016). Isomerization of n-hexane over Pt-H3PW12O40/SBA-15 bifunctional catalysts: Effect of the preparation method on catalytic performance. *Applied Catalysis A: General*, 528, 44-51.
- Polshettiwar, V., Cha, D., Zhang, X., & Basset, J. M. (2010). High-surface-area silica nanospheres (KCC-1) with a fibrous morphology. *Angewandte Chemie International Edition*, 49(50), 9652-9656.
- Popova, M., Lazarova, H., Kalvachev, Y., Todorova, T., Szegedi, Á., Shestakova, P., Mali, G., Dasireddy, V.D. & Likozar, B. (2017). Zr-modified hierarchical mordenite as heterogeneous catalyst for glycerol esterification. *Catalysis Communications*, 100, 10-14.
- Pradhan, S., Madankar, C. S., Mohanty, P., & Naik, S. N. (2012). Optimization of reactive extraction of castor seed to produce biodiesel using response surface methodology. *Fuel*, 97, 848-855.
- Prapainainar, P., Maliwan, S., Sarakham, K., Du, Z., Prapainainar, C., Holmes, S. M., & Kongkachuichay, P. (2018). Homogeneous polymer/filler composite membrane by spraying method for enhanced direct methanol fuel cell performance. *International Journal of Hydrogen Energy*, 43(31), 14675-14690.
- Prapainainar, P., Pattanapisutkun, N., Prapainainar, C., & Kongkachuichay, P. (2019). Incorporating graphene oxide to improve the performance of Nafion-mordenite composite membranes for a direct methanol fuel cell. *International Journal of Hydrogen Energy*, 44(1), 362-378.
- Primo, A., & Garcia, H. (2014). Zeolites as catalysts in oil refining. *Chemical society reviews*, 43(22), 7548-7561.
- Prins, R. (2012). Hydrogen spillover. Facts and fiction. *Chemical reviews*, 112(5), 2714-2738.
- Qiu, S., Wang, T., & Fang, Y. (2019). High-efficient preparation of gasoline-ranged C5–C6 alkanes from biomass-derived sugar polyols of sorbitol over Ru-MoO<sub>3</sub>-x/C catalyst. *Fuel Processing Technology*, 183, 19-26.
- Rahimi, N., & Karimzadeh, R. (2011). Catalytic cracking of hydrocarbons over modified ZSM-5 zeolites to produce light olefins: A review. *Applied Catalysis A: General*, 398(1-2), 1-17.

- Rankovic, N., Bourhis, G., Loos, M., & Dauphin, R. (2015). Understanding octane number evolution for enabling alternative low RON refinery streams and octane boosters as transportation fuels. *Fuel*, *150*, 41-47.
- Ren, S., Gong, C., Zeng, P., Guo, Q., & Shen, B. (2016). Synthesis of flammulina-like mordenite using starch as template and high catalytic performance in crack of wax oil. *Fuel*, *166*, 347-351.
- Rojo-Gama, D., Signorile, M., Bonino, F., Bordiga, S., Olsbye, U., Lillerud, K. P., Beato, P. & Svelle, S. (2017). Structure–deactivation relationships in zeolites during the methanol–to-hydrocarbons reaction: Complementary assessments of the coke content. *Journal of Catalysis*, *351*, 33-48.
- Roldán, R., Romero, F. J., Jiménez-Sanchidrián, C., Marinas, J. M., & Gómez, J. P. (2005). Influence of acidity and pore geometry on the product distribution in the hydroisomerization of light paraffins on zeolites. *Applied Catalysis A: General*, *288*(1-2), 104-115.
- Saada, R., AboElazayem, O., Kellici, S., Heil, T., Morgan, D., Lampronti, G. I., & Saha, B. (2018). Greener synthesis of dimethyl carbonate using a novel tin-zirconia/graphene nanocomposite catalyst. *Applied Catalysis B: Environmental*, *226*, 451-462.
- Sabyrov, K., Musselwhite, N., Melaet, G., & Somorjai, G. A. (2017). Hydroisomerization of n-hexadecane: remarkable selectivity of mesoporous silica post-synthetically modified with aluminum. *Catalysis Science & Technology*, *7*(8), 1756-1765.
- Sankar, E. S., Mohan, V., Suresh, M., Saidulu, G., Raju, B. D., & Rao, K. R. (2016). Vapor phase esterification of levulinic acid over ZrO<sub>2</sub>/SBA-15 catalyst. *Catalysis Communications*, *75*, 1-5.
- Sano, T., Wakabayashi, S., Oumi, Y., & Uozumi, T. (2001). Synthesis of large mordenite crystals in the presence of aliphatic alcohol. *Microporous and Mesoporous Materials*, *46*(1), 67-74.
- Saxena, S. K., Viswanadham, N., & Garg, M. O. (2013). Cracking and isomerization functionalities of bi-metallic zeolites for naphtha value upgradation. *Fuel*, *107*, 432-438.
- Sazama, P., Kaucky, D., Moravkova, J., Pilar, R., Klein, P., Pastvova, J., Tabor, E., Sklenak, S., Jakubec, I & Mokrzycki, L. (2017). Superior activity of non-

- interacting close acidic protons in Al-rich Pt/H-\* BEA zeolite in isomerization of n-hexane. *Applied Catalysis A: General*, 533, 28-37.
- Sazama, P., Pastvova, J., Kaucky, D., Moravkova, J., Rathousky, J., Jakubec, I., & Sadvovska, G.. (2018). Does hierarchical structure affect the shape selectivity of zeolites? Example of transformation of n-hexane in hydroisomerization. *Journal of Catalysis*, 364, 262-270.
- Sazegar, M. R., Mahmoudian, S., Mahmoudi, A., Triwahyono, S., Jalil, A. A., Mukti, R. R., Kamarudin, N.H.N. & Ghoreishi, M. K. (2016). Catalyzed Claisen–Schmidt reaction by protonated aluminate mesoporous silica nanomaterial focused on the (E)-chalcone synthesis as a biologically active compound. *RSC Advances*, 6(13), 11023-11031.
- Schwieger, W., Machoke, A. G., Weissenberger, T., Inayat, A., Selvam, T., Klumpp, M., & Inayat, A. (2016). Hierarchy concepts: classification and preparation strategies for zeolite containing materials with hierarchical porosity. *Chemical Society Reviews*, 45(12), 3353-3376.
- Setiabudi, H. D., Jalil, A. A., & Triwahyono, S. (2012a). Ir/Pt-HZSM5 for n-pentane isomerization: Effect of iridium loading on the properties and catalytic activity. *Journal of Catalysis*, 294, 128-135.
- Setiabudi, H. D., Jalil, A. A., Triwahyono, S., Kamarudin, N. H. N., & Mukti, R. R. (2012b). IR study of iridium bonded to perturbed silanol groups of Pt-HZSM5 for n-pentane isomerization. *Applied Catalysis A: General*, 417, 190-199.
- Setiabudi, H. D., Jalil, A. A., Triwahyono, S., Kamarudin, N. H. N., & Jusoh, R. (2013). Ir/Pt-HZSM5 for n-pentane isomerization: Effect of Si/Al ratio and reaction optimization by response surface methodology. *Chemical Engineering Journal*, 217, 300-309.
- Shahul Hamid, M. Y., Triwahyono, S., Jalil, A. A., Che Jusoh, N. W., Izan, S. M., & Tuan Abdullah, T. A. (2018). Tailoring the properties of metal oxide loaded/KCC-1 toward a different mechanism of CO<sub>2</sub> methanation by in situ IR and ESR. *Inorganic Chemistry*, 57(10), 5859-5869.
- Shakun, A. N., & Fedorova, M. L. (2014). Isomerization of light gasoline fractions: The efficiency of different catalysts and technologies. *Catalysis in Industry*, 6(4), 298-306.



- Shami, S., Dash, R. R., Verma, A. K., Dash, A. K., & Pradhan, A. (2019). Adsorptive Removal of Surfactant using Dolochar: A Kinetic and Statistical Modeling Approach. *Water Environment Research*.
- Sharma, P., Yeo, J. G., Kim, D. K., & Cho, C. H. (2012). Organic additive free synthesis of mesoporous naoncrystalline NaA zeolite using high concentration inorganic precursors. *Journal of Materials Chemistry*, 22(7), 2838-2843.
- Shiokawa, K., Ito, M., & Itabashi, K. (1989). Crystal structure of synthetic mordenites. *Zeolites*, 9(3), 170-176.
- Sie, S. T. (1993). Acid-catalyzed cracking of paraffinic hydrocarbons. 3. Evidence for the protonated cyclopropane mechanism from hydrocracking/hydroisomerization experiments. *Industrial & Engineering Chemistry Research*, 32(3), 403-408.
- Sidik, S. M., Jalil, A. A., Triwahyono, S., Abdullah, T. A. T., & Ripin, A. (2015). CO<sub>2</sub> reforming of CH<sub>4</sub> over Ni/mesostructured silica nanoparticles (Ni/MSN). *RSC Advances*, 5(47), 37405-37414.
- Song, C., Wang, M., Zhao, L., Xue, N., Peng, L., Guo, X., Ding, W., Yang, W. & Xie, Z. (2013). Synergism between the Lewis and Brønsted acid sites on HZSM-5 zeolites in the conversion of methylcyclohexane. *Chinese Journal of Catalysis*, 34(11), 2153-2159.
- Stradling, R., Williams, J., Hamje, H., & Rickeard, D. (2016). Effect of octane on performance, energy consumption and emissions of two Euro 4 passenger cars. *Transportation Research Procedia*, 14, 3159-3168.
- Tamizhduraia, P., Rameshb, A., Santhana, P. K., Narayananc, S., Shanthib, K., Sivasankera, S. (2019). *Microporous and Mesoporous Materials*, 287, 192–202.
- Tang, B., Dai, W., Sun, X., Guan, N., Li, L., & Hunger, M. (2014). A procedure for the preparation of Ti-Beta zeolites for catalytic epoxidation with hydrogen peroxide. *Green Chemistry*, 16(4), 2281-2291.
- Tang, B., Song, W. C., Li, S. Y., Yang, E. C., & Zhao, X. J. (2018). Post-synthesis of Zr-MOR as a robust solid acid catalyst for the ring-opening aminolysis of epoxides. *New Journal of Chemistry*, 42(16), 13503-13511.
- Teh, L. P., Triwahyono, S., Jalil, A. A., Firmansyah, M. L., Mamat, C. R., & Majid, Z. A. (2016). Fibrous silica mesoporous ZSM-5 for carbon monoxide methanation. *Applied Catalysis A: General*, 523, 200-208.

- Teh, L. P., Triwahyono, S., Jalil, A. A., Mukti, R. R., Aziz, M. A. A., & Shishido, T. (2015). Mesoporous ZSM5 having both intrinsic acidic and basic sites for cracking and methanation. *Chemical Engineering Journal*, 270, 196-204.
- Thommes, M., Kaneko, K., Neimark, A. V., Olivier, J. P., Rodriguez-Reinoso, F., Rouquerol, J., & Sing, K. S. (2015). Physisorption of gases, with special reference to the evaluation of surface area and pore size distribution (IUPAC Technical Report). *Pure and Applied Chemistry*, 87(9-10), 1051-1069.
- Triwahyono, S., Jalil, A. A., Izan, S. M., Jamari, N. S., & Fatah, N. A. A. (2019). Isomerization of linear C5–C7 over pt loaded on protonated fibrous silica@ Y zeolite (Pt/HSi@ Y). *Journal of Energy Chemistry*, 37, 163-171.
- Triwahyono, S., Jalil, A. A., & Hattori, H. (2007). Study of hydrogen adsorption on Pt/WO<sub>3</sub>-ZrO<sub>2</sub> through Pt sites. *Journal of Natural Gas Chemistry*, 16(3), 252-257.
- Triwahyono, S., Jalil, A. A., Timmiati, S. N., Ruslan, N. N., & Hattori, H. (2010). Kinetics study of hydrogen adsorption over Pt/MoO<sub>3</sub>. *Applied Catalysis A: General*, 372(1), 103-107.
- Triwahyono, S., Jalil, A. A., Mukti, R. R., Musthofa, M., Razali, N. A. M., & Aziz, M. A. A. (2011). Hydrogen spillover behavior of Zn/HZSM-5 showing catalytically active protonic acid sites in the isomerization of n-pentane. *Applied Catalysis A: General*, 407(1-2), 91-99.
- Triwahyono, S., Jalil, A. A., & Musthofa, M. (2010). Generation of protonic acid sites from pentane on the surfaces of Pt/SO<sub>4</sub><sup>2-</sup>-ZrO<sub>2</sub> and Zn/H-ZSM5 evidenced by IR study of adsorbed pyridine. *Applied Catalysis A: General*, 372(1), 90-93.
- Triwahyono, S., Yamada, T., & Hattori, H. (2003a). Effects of Na Addition, Pyridine Preadsorption, and Water Preadsorption on the Hydrogen Adsorption Property of Pt/SO<sub>4</sub><sup>2-</sup>-ZrO<sub>2</sub>. *Catalysis Letters*, 85(1-2), 109-115.
- Triwahyono, S., Yamada, T., & Hattori, H. (2003b). IR study of acid sites on WO<sub>3</sub>-ZrO<sub>2</sub>. *Applied Catalysis A: General*, 250(1), 75-81.
- Triwahyono, S., Yamada, T., & Hattori, H. (2003c). IR study of acid sites on WO<sub>3</sub>-ZrO<sub>2</sub> and Pt/WO<sub>3</sub>-ZrO<sub>2</sub>. *Applied Catalysis A: General*, 242(1), 101-109.
- Triwahyono, S., Salamun, N., Jalil, A. A., Izan, S. M., Setiabudi, H. D., & Prasetyoko, D (2018). Zirconium-loaded mesostructured silica nanoparticles adsorbent for

- removal of hexavalent chromium from aqueous solution. *Industrial & Engineering Chemistry Research*, 58(2), 704-712.
- Uhlig, H., Muenster, T., Kloess, G., Ebbinghaus, S. G., Einicke, W. D., Gläser, R., & Enke, D. (2018). Synthesis of MCM-48 granules with bimodal pore systems via pseudomorphic transformation of porous glass. *Microporous and Mesoporous Materials*, 257, 185-192.
- Qu, Q., Li, W., & Wu, Q. (2019). Formation Mechanism of Silica Particles with Dendritic Structure. *ChemistrySelect*, 4(21), 6656–6661.
- Vajglova, Z., Kumar, N., Peurla, M., Hupa, L., Semikin, K., Sladkovskiy, D. A., & Murzin, D. Y. (2019). Effect of the preparation of Pt-modified zeolite Beta-bentonite extrudates on their catalytic behaviour in n-hexane hydroisomerization. *Industrial & Engineering Chemistry Research*.
- Verboekend, D., & Pérez-Ramírez, J. (2014). Cover Picture: Towards a Sustainable Manufacture of Hierarchical Zeolites (ChemSusChem 3/2014). *ChemSusChem*, 7(3), 651-651.
- Viswanadham, N., Saxena, S. K., & Garg, M. O. (2013). Octane number enhancement studies of naphtha over noble metal loaded zeolite catalysts. *Journal of Industrial and Engineering Chemistry*, 19(3), 950-955.
- Wang, H., Meng, X., Zhao, G., & Zhang, S. (2017). Isobutane/butene alkylation catalyzed by ionic liquids: a more sustainable process for clean oil production. *Green Chemistry*, 19(6), 1462-1489.
- Wang, W., Liu, C. J., & Wu, W. (2019). Bifunctional catalysts for the hydroisomerization of n-alkanes: the effects of metal-acid balance and textural structure. *Catalysis Science & Technology*.
- Weitkamp, J., & Traa, Y. (1999). Isobutane/butene alkylation on solid catalysts. Where do we stand? *Catalysis Today*, 49(1-3), 193-199.
- Williams, B. A., Babitz, S. M., Miller, J. T., Snurr, R. Q., & Kung, H. H. (1999). The roles of acid strength and pore diffusion in the enhanced cracking activity of steamed Y zeolites. *Applied Catalysis A: General*, 177(2), 161-175.
- Xing, Y., Du, X., Li, X., Huang, H., Li, J., Wen, Y., & Zhang, X. (2018). Tunable dendrimer-like porous silica nanospheres: Effects of structures and stacking manners on surface wettability. *Journal of Alloys and Compounds*, 732, 70-79.
- Yang, E., Jang, E. J., Lee, J. G., Yoon, S., Lee, J., Musselwhite, N., Kwak, J.H. & An, K. (2018). Acidic effect of porous alumina as supports for Pt nanoparticle

- catalysts in n-hexane reforming. *Catalysis Science & Technology*, 8(13), 3295-3303.
- Yang, L., Wang, W., Song, X., Bai, X., Feng, Z., Liu, T., & Wu, W. (2019). The hydroisomerization of n-decane over Pd/SAPO-11 bifunctional catalysts: The effects of templates on characteristics and catalytic performances. *Fuel Processing Technology*, 190, 13-20.
- Yang, Z., Liu, Y., Zhao, J., Gou, J., Sun, K., Liu, C. (2017). Zinc-modified Pt/SAPO-11 for improving the isomerization selectivity to dibranched alkanes. *Chinese Journal of Catalysis*, 38, 509–517.
- Yu, Q., Cui, C., Zhang, Q., Chen, J., Li, Y., Sun, J., Li, C., Cui, Q., Yang, C. and Shan, H. (2013). Hierarchical ZSM-11 with intergrowth structures: Synthesis, characterization and catalytic properties. *Journal of Energy Chemistry*, 22(5), 761–768.
- Zhang, F., Wang, Z., Xu, K. Q., Xia, J., Liu, Q., & Wang, Z. (2018b). Highly dispersed ultrafine Pt nanoparticles on nickel-cobalt layered double hydroxide nanoarray for enhanced electrocatalytic methanol oxidation. *International Journal of Hydrogen Energy*, 43(33), 16302-16310.
- Zhang, H., Yang, W., Roslan, I. I., Jaenicke, S., & Chuah, G. K. (2019b). A combo Zr-HY and Al-HY zeolite catalysts for the one-pot cascade transformation of biomass-derived furfural to  $\gamma$ -valerolactone. *Journal of Catalysis*, 375, 56-67.
- Zhang, K., & Ostraat, M. L. (2016). Innovations in hierarchical zeolite synthesis. *Catalysis Today*, 264, 3-15.
- Zhang, P., Liu, H., Yue, Y., Zhu, H., & Bao, X. (2018a). Direct synthesis of hierarchical SAPO-11 molecular sieve with enhanced hydroisomerization performance. *Fuel Processing Technology*, 179, 72-85.
- Zhang, Y., Liu, D., Men, Z., Huang, K., Lv, Y., Li, M., & Lou, B. (2019a). Hydroisomerization of n-dodecane over bi-porous Pt-containing bifunctional catalysts: Effects of alkene intermediates' journey distances within the zeolite micropores. *Fuel*, 236, 428-436.
- Zhang, Y., Zhao, R., Sanchez-Sanchez, M., Haller, G. L., Hu, J., Bermejo-Deval, R., Liu, Y. & Lercher, J. A. (2019c). Promotion of protolytic pentane conversion on H-MFI zeolite by proximity of extra-framework aluminum oxide and Brønsted acid sites. *Journal of Catalysis*, 370, 424-433.



## APPENDIX A

### Calculation of Percentage of Platinum (Pt) and Zirconium (Zr)

Taking the amount of catalyst HM@KCC-1 as 1g and 0.5 wt% of Pt as desired amount of Pt, the calculation was as follows,

Mass of Pt needed,

$$0.5\text{wt}\% \text{ Pt} = \frac{x \text{ g Pt}}{1 \text{ g HM@KCC-1} + x \text{ g Pt}}$$

$$x \text{ g Pt} = 5.025 \times 10^{-3} \text{ g Pt}$$

With MW Pt = 195.084 g mole<sup>-1</sup> and MW Pt solution = 517.9 g mole<sup>-1</sup>

Mole of Pt needed,

$$\begin{aligned} \text{g Pt solution} &= \frac{517.9 \text{ g mole}^{-1} \text{ Pt solution} \times 5.025 \times 10^{-3} \text{ g Pt}}{195.084 \text{ g mole}^{-1} \text{ Pt}} \\ &= 1.3340 \times 10^{-2} \text{ g Pt solution} \end{aligned}$$

With concentration of Pt solution = 9.6782 g/ 100 mL

Volume of Pt needed,

$$\begin{aligned} \text{mL Pt solution} &= \frac{1.3340 \times 10^{-2} \text{ g Pt solution}}{9.6782 \text{ g/ 100 mL}} \\ &= 0.1378 \text{ mL Pt solution} \end{aligned}$$

Thus, 0.1378 mL of Pt solution is needed to prepare 0.5 wt% Pt on 1 g HM@KCC-1.

Taking the amount of HM@KCC-1 as 1g and 5 wt % of Zr, the calculation is as follows,

Mass of Zr needed,

Mass of Pt needed,

$$5 \text{ wt\% Zr} = \frac{x \text{ g Zr}}{1 \text{ g HM@KCC-1} + x \text{ g Zr}}$$

$$x \text{ g Zr} = 0.0526 \text{ g Zr}$$

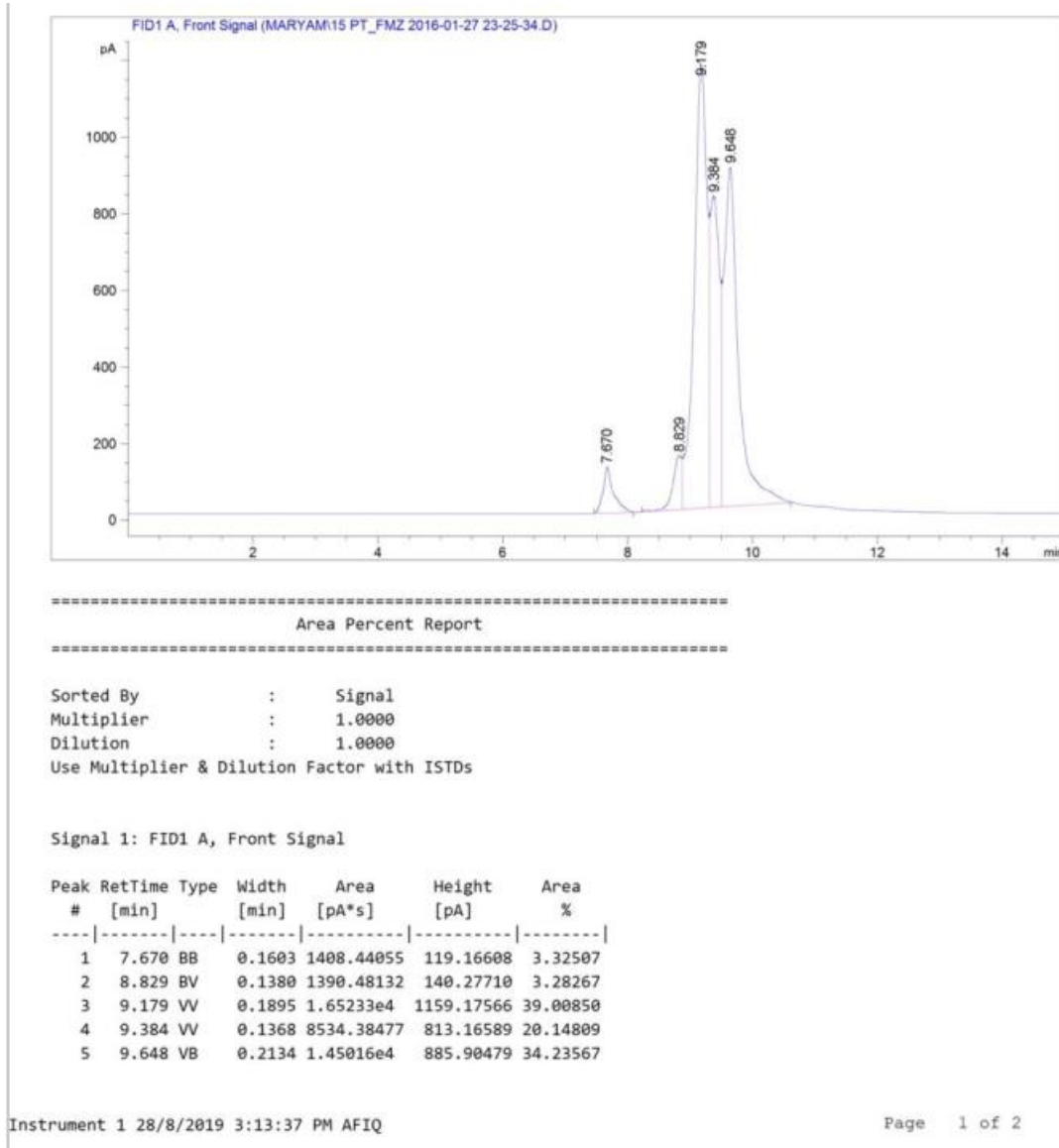
With MW Zr = 91.224 g mole<sup>-1</sup> and MW ZrOCl<sub>2</sub>.H<sub>2</sub>O = 322.252 g mole<sup>-1</sup>

$$\begin{aligned} \text{g ZrOCl}_2\cdot\text{H}_2\text{O} &= \frac{322.252 \text{ g mole}^{-1} \text{ ZrOCl}_2\cdot\text{H}_2\text{O}}{91.224 \text{ g mole}^{-1} \text{ Zr}} \times 0.0526 \text{ g Zr} \\ &= 0.1858 \text{ g ZrOCl}_2\cdot\text{H}_2\text{O} \end{aligned}$$

Thus, mass of ZrOCl<sub>2</sub>.H<sub>2</sub>O needed to prepare 5 wt% Zr on 1 g HM@KCC-1 is 0.1858 g ZrOCl<sub>2</sub>.H<sub>2</sub>O .

## Appendix B

### Raw Data For *n*-Hexane Hydroisomerization





## Appendix C

### Calculation for Catalytic Activity

Based on the raw data in Appendix B, the calculation of conversion, selectivity and yield of a particular product was calculated as below:

$X_{n\text{-hexane}}$

$$= \frac{1408.4+1390.5+16523.3+8534.4}{1408.4+1390.5+16523.3+8534.4+14501.6} \times 100$$

$$= 66\%$$

Selectivity of isomer was calculated as follows:

$$= \frac{1390.5+16523.3+8534.4}{1408.4+1390.5+16523.3+8534.4+14501.6} \times 100$$

$$= 95\%$$

And the yield,

$$= \frac{66 \times 95}{100}$$

$$= 63\%$$

## Appendix D

### Kinetic study

#### Calculation of Rate Constant, K

The rate constant, k was calculated according to the following equation:

$$k = \frac{\text{no. of mole } n\text{-hexane (mole)}}{\text{Weight of catalyst (g) x time of pulse (s}^{-1}\text{) x surface area}}$$

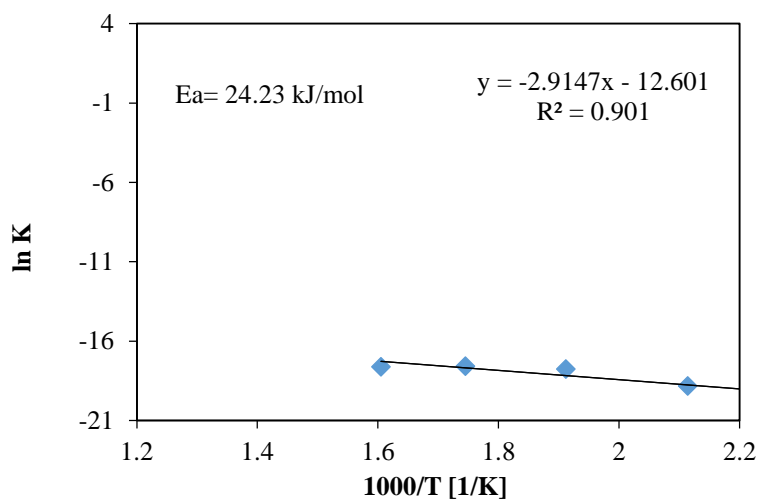
With the mole of *n*-hexane =  $6.83 \times 10^{-6}$ , the value of surface area is  $679 \text{ m}^2/\text{g}$  presented in Table 4.2, the weight of 5ZrHM@KCC-1 = 0.1 g, and by assuming the time of pulse per second is 1, the rate constant for 5ZrHM@KCC-1:

$$k = \frac{6.83 \times 10^{-6} \text{ (mole)}}{0.1 \text{ (g) x } 1 \text{ (s}^{-1}\text{) x } 679 \text{ m}^2/\text{g}} = 3.638 \times 10^{-8} \text{ mole g}^{-1} \text{ s}$$

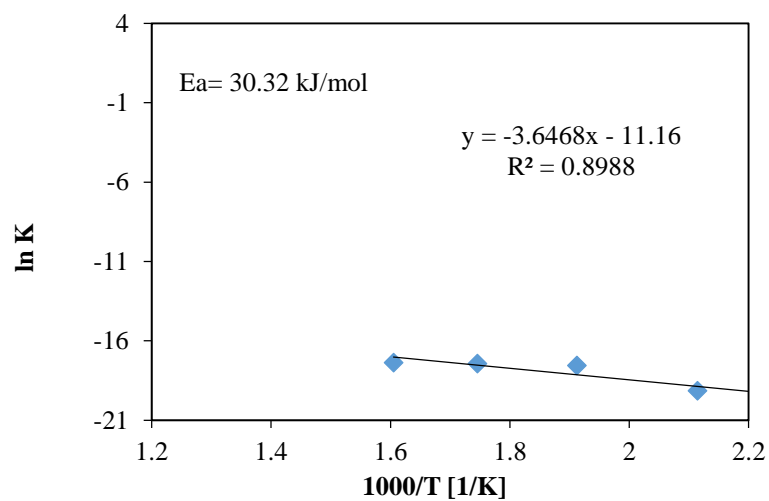
Thus, the rate constant of 5ZrHM@KCC-1 was  $3.638 \times 10^{-8} \text{ mole g}^{-1} \text{ s}$

## Arrhenius Plot

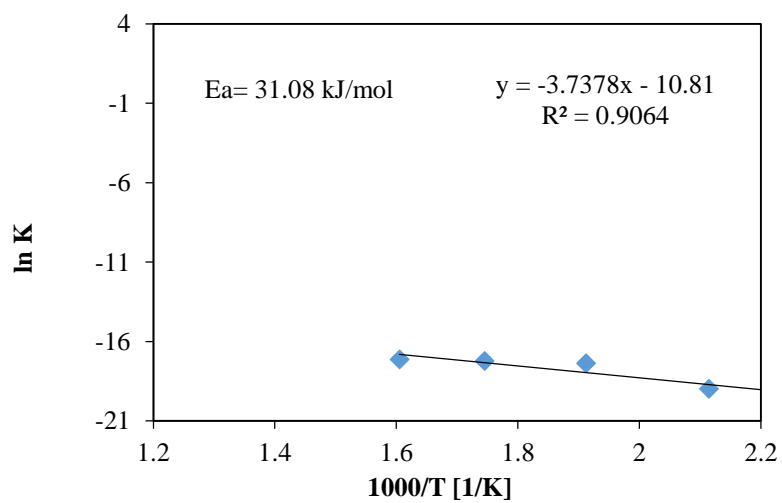
**1Zr/HM@KCC-1(150-350 °C)**



**5Zr/HM@KCC-1 (150-350 C)**



**10Zr/HM@KCC-1 (150-350 C)**



## Appendix E

### Calculation of Acid Sites Concentration

The amount of pyridine per gram of catalyst was calculated using integrated molar extinction coefficient (IMEC), 1.67 cm/ $\mu$ mole and 2.22 cm/ $\mu$ mole for Brönsted acid sites and Lewis acid sites respectively.

$$\emptyset = \frac{[\text{IA (B)}/\text{IMEC (B)} + \text{IA (L)}/\text{IMEC (L)}]}{(3.14 R^2)} = \frac{C_{\text{py}}}{(3.14 R^2)}$$

The amount of pyridine per gram catalyst (C) was obtained by dividing  $\emptyset$  by the weight per  $\text{cm}^2$  disk

$$C_{\text{B}} (\text{pyridine on Brönsted acid sites}) = \frac{1.88 \text{ IA(B)} R^2}{W}$$

$$C_{\text{L}} (\text{pyridine on Lewis acid sites}) = \frac{1.42 \text{ IA(L)} R^2}{W}$$

With Brönsted integrated peak area at  $1545 \text{ cm}^{-1}$  of HM@KCC-1 = 0.15625 and Lewis acid sites integrated peak area at  $1445 \text{ cm}^{-1}$  of HM@KCC-1 = 0.48415. The calculation was made as follows,

$$C_{\text{B}} = \frac{1880 \mu\text{mole} \times 0.15625 \times (2 \text{ cm})^2}{25 \text{ mg}}$$

$$= 46.92 \mu\text{mole/g}$$

$$C_{\text{L}} = \frac{1420 \mu\text{mole} \times 0.48415 \times (2 \text{ cm})^2}{25 \text{ mg}}$$

$$= 110.12 \mu\text{mole/g}$$

Thus, the Brönsted and Lewis acid sites acid sites concentration for HM@KCC-1 are  $47 \mu\text{mole/g}$  and  $110 \mu\text{mole/g}$ , respectively.

## Appendix F

### Microcatalytic pulse reactor experimental set-up



## Appendix G

### Calculation of g-value

The g-value was calculated based on the energy absorbed in terms of Bohr magneton as given in the equation below:

$$E = h\nu = g B_N H$$

$$g = h\nu/B_N H$$

Where

$$B_N = \text{Bohr magneton} = 9.27 \times 10^{-24} \text{ JT}^{-1} = 9.27 \times 10^{-27} \text{ J/mT}$$

$$H = \text{Magnetic field strength} = 336.977 \text{ mT}$$

$$h = \text{Planck's constant} = 6.626 \times 10^{-34} \text{ Js}$$

$$\nu = \text{frequency of radiation} = 9.015 \text{ GHz} \times 1000 = 9015 \text{ MHz} = 9015 \times 10^6 \text{ s}^{-1}$$

g = g value

$$g = 6.626 \times 10^{-34} \text{ Js} \times 9015 \times 10^6 \text{ s}^{-1} / 9.27 \times 10^{-27} \text{ J/mT} \times 336.977 \text{ mT}$$

$$g = 1.91$$

## Appendix H

### Calculation for mass transfer parameter

The mass transfer parameters were evaluated based on the following equations:

#### Porosity, $\varepsilon$

$$\varepsilon = \frac{V_p}{V_{cat}} \quad (1)$$

Where  $V_p$  is catalyst pore volume ( $m^3$ ) and  $V_{cat}$  is catalyst volume ( $m^3$ )

#### Tortuosity, $\tau$

$$\tau = 1 - 0.5 \ln(1 - \varepsilon) \quad (2)$$

#### Molecular diffusivity, $D_{AB(673\text{ K})}$

$$D_{AB(673\text{ K})} = D_{AB(298\text{ K})} \left( \frac{673}{298} \right)^{1.75} \quad (3)$$

#### Thiele modulus

$$\phi_1 = R_p \sqrt{\frac{k_1 \rho_c S_a}{D_{eff}}} \quad (4)$$

Where  $R_p$  is the catalyst radius (m),  $k_1$  is the specific reaction rate (m/s),  $\rho_c$  is the catalyst density ( $g/m^3$ ),  $S_a$  is the catalyst surface area ( $m^2/g$ ) and  $D_{eff}$  is the effective diffusivity.

#### Effective diffusivity:

$$D_{eff} = \frac{\varepsilon}{\tau} D_{AB} \quad (5)$$

#### Internal effectiveness factor:

$$\eta = \frac{3}{\phi_1^2} \left( \phi_1 \left( \frac{e^{\phi_1} + e^{-\phi_1}}{e^{\phi_1} - e^{-\phi_1}} \right) - 1 \right) \quad (6)$$

#### Weiz-Prater Criterion:

$$C_{WP} = \eta \phi_1^2 = 3(\phi_1 \coth \phi_1 - 1) \quad (7)$$

For  $C_{WP} < 1$  implies internal diffusion limitation is negligible and vice-versa

## LIST OF PUBLICATIONS

### Journal with Impact Factor

1. **Ibrahim, M.**, Jalil, A.A., Triwahyono, S., Khusnun, N.F., Fatah, N.A.A., Hamid, M. Y. S., Gambo, Y., Abdulrasheed, A. A., Hassan N.S., and Mohamed, M. (2019). Enhanced *n*-Hexane Hydroisomerization Over Bicontinuous Lamellar Silica Mordenite Supported Platinum (Pt/HM@KCC-1) Catalyst. *International Journal of Hydrogen Energy*, doi.org/10.1016/j.ijhydene.2019.04.067.(Q2, IF: 4.084)

### Non-Indexed Conference Proceedings

1. **Ibrahim, M.**, Jalil, A.A., Triwahyono, S., Khusnun, N.F., Tuned acidic properties of fibrous mordenite zeolite for *n*-hexane isomerization. *4th International Conference of Chemical Engineering & Industrial Biotechnology*, Kuala Lumpur, Malaysia, 1-2 August 2018.
2. **Ibrahim, M.**, Jalil, A.A., Triwahyono, S., Fatah, N.A.A., Izan S.M., and Teh, L.P. Preparation of fibrous mordenite based catalyst for *n*-hexane isomerization. *5th Conference on Emerging Energy and Process Technology (CONCEPT)*, Negeri Sembilan, Malaysia, 7-8 December 2016.
3. **Ibrahim, M.**, Jalil, A.A., Triwahyono, S., Khusnun, N.F. Silica modified mordenite zeolite for *n*-pentane isomerization: synthesis and catalytic reaction. *International Conference on Catalysis (ICAT)*, Johor Bahru, Malaysia, 20-21 September 2016.
4. **Ibrahim, M.**, Jalil A.A., and Triwahyono, S. A review on catalytic CO<sub>2</sub> methanation for high calorie hydrocarbon. *4th Conference Emerging Energy & Process Technology (CONCEPT)*, Melaka, Malaysia, 15-16 December 2015.